Thermomechanical structure of European continental lithosphere: constraints from rheological profiles and EET estimates

Cloetingh, S.A.P.L.; Burov, E.B.

published in
Geophysical Journal International
1996

DOI (link to publisher)
10.1111/j.1365-246X.1996.tb05633.x

document version
Publisher's PDF, also known as Version of record

Geophys. J. Int. (1996) **124,** 695–723

Thermomechanical structure of European continental lithosphere: constraints from rheological profiles and EET estimates

Sierd Cloetingh[1] and Evgene B. Burov[2]

[1] *Institute of Earth Sciences, De Boelelaan* 1085 *Vrije Universiteit* 1081 *HV Amsterdam, The Netherlands*
[2] *Institut de Physique du Globe de Paris,* 4 *Place Jussieu,* 75252 *Paris Cedex* 05 *France*

Accepted 1995 September 11. Received 1995 July 18; in original form 1994 October 24

SUMMARY

The EET (equivalent elastic thickness) of the lithosphere is a measure of the integrated lithospheric strength. It is directly related to the mechanical thickness and rheology of the crustal and mantle lithosphere. We present a comparison of EET estimates and strength profiles based on the extrapolation of rock mechanics data for different parts of the European and Eurasian continental lithosphere. We discuss the temporal and spatial variations in the mechanical thickness and strength inferred from data for Precambrian segments of Europe's lithosphere, Variscan Europe and the Alpine collision belt. This analysis demonstrates important spatial and temporal variations in lithospheric rigidity for orogenic belts and sedimentary basins in eastern and western Europe and Asian parts of Eurasia. The EET estimates based on synthetic rheological profiles constrained by newly available geophysical data are consistent with the estimates of EET derived from flexural studies of sedimentary basins, forelands and orogenic belts. These rheological profiles suggest weakening of the major parts of the European and Eurasian continental lithosphere by decoupling of the crustal and upper-mantle parts. A comparison with the seismicity–depth distribution for some selected sites suggests that the intra-plate seismicity is essentially restricted to the upper crustal parts of Europe's lithosphere, providing additional support to the notion of the decoupled lithosphere. The presence of intra-plate stress fields can explain a significant part of the observed variations in EET estimates within individual thermotectonic age groups. A comparison of wavelengths of crustal and lithospheric folding with observations shows these wavelengths to be consistent with estimates of EET inferred from the rheological response of basins and orogens at more moderate levels of intra-plate stress.

Key words: Flexure of the lithosphere, focal depth, lithospheric deformation, Moho discontinuity, rheology, tectonics.

1 INTRODUCTION

Over the last decade, studies of the continental lithosphere have considerably enhanced insights into the thermomechanical evolution of the continents. In the first few years of the decade, these studies focused on obtaining EET estimates from flexure of the continental lithosphere and vertical loads (e.g. Cochran 1980; Sibson 1982; Meissner & Strehlau 1982; Lyon-Caen & Molnar 1983, 1984; Karner, Steckler & Thorne 1983; Karner & Watts 1983; Sheffels & McNutt 1986). Later investigations of the data of rock mechanics and the rheological composition of the continents have allowed studies on the relationship between EET and rheology (Kusznir & Karner 1985; Kusznir & Park 1987; Kusznir & Matthews 1988; De Rito, Cozzarelli & Hodge 1986; McNutt, Diament & Kogan 1988; Watts 1992). However, these earlier studies failed to propose a unique model that could allow an interpretation of the lithospheric structure on the basis of EET estimates, as developed earlier for the oceanic lithosphere (Wallcott 1970; Watts, Bodine & Steckler 1980a; Watts, Bodine & Ribe 1980b). In the oceans, EET can be directly related to the age of the lithosphere, or more specifically to the depth to a geotherm (450–600 °C), which is generally controlled by the age. Similarly, the cut-off depth of oceanic intraplate seismicity was shown to be limited by an isotherm of 750 °C (Wiens & Stein 1983), consistent with predictions from experimental studies of rock mechanics (see also Bodine, Steckler & Watts 1981). Thus it appears that the mechanical properties of the oceanic lithosphere are largely consistent with inferences from the plate-cooling model (Parsons & Sclater 1977). The thermal

age of the oceanic lithosphere is also well constrained on the basis of independent data such as data on palaeomagnetic anomalies or heat flux (Sclater, Parsons & Jaupart 1981). Deviations of oceanic EET from this general age–EET dependence are usually explained by the presence of local thermal anomalies or, in certain cases, by high flexural stress that can also reduce the integrated plate strength (e.g. Bodine *et al.* 1981; Wessel 1993).

The general problem with the treatment of continental EET estimates is that the rheological structure of the continents is intrinsically more complex than that in the oceans. As their tectonic history is also much longer, uncertainties resulting from the extrapolation of the data of rock mechanics experiments to geologically relevant temporal and spatial scales are much larger. The thermal history and thermal structure of the continents are also much less constrained, and deep seismic data have revealed a long-lasting heritage of a complex geological evolution on deep density/thermal structures, associated with, for example, ancient plate boundaries (Zielhuis & Nolet 1994). It is also obvious that the complex multilayered rheology structure might possibly lead to some specific mechanical effects such as the presence of intra-lithospheric decoupling zones. More recently, the depth-dependent rheological structure of the continental lithosphere has been addressed by the construction of the strength profiles extrapolated from the rock mechanics data, and additionally constrained by multidisciplinary analysis of the evolution of different regions. Such multidisciplinary approaches allow us to test experimental rheology data against independent data from, for example, seismicity, gravity, thermal flux, topography, petrology, and magnetotelluric studies. Integration of these approaches enabled a more complete treatment of EET estimates in terms of the rheological structure (Burov & Diament 1992; Ranalli 1994). More recently, Burov & Diament (1995) proposed a unified oceanic continental model of the lithosphere that relates EET and three major estimable parameters such as thermal age, crustal thickness and curvature of bending.

The major difference between the rheological structures of the continental and oceanic lithospheres is caused by the presence of a thick continental crust that is 4–5 times thicker than the normal oceanic crust. A typical value for the thickness of the continental crust is about 35–40 km, which is comparable or even greater than the thickness of the mechanical mantle lithosphere [the latter is commonly defined as the depth interval between the Moho and the depth to the 750 °C isotherm (e.g. McNutt *et al.* 1988)]. The thermo-mechanical properties of the continental crust are controlled by mineral compositions which are significantly different from those of the mantle lithosphere. Consequently, to understand the mechanical behaviour of the continental lithosphere, it is vital to account for the crustal rheology. In contrast with the upper mantle, the continental crust can be very variable in composition (e.g. Meissner & Strehlau 1982; Meissner 1986; Meissner, Wever & Flüh 1987; Kirby & Kronenberg 1987a,b; Banda & Cloetingh 1992; Cloetingh & Banda 1992). Whereas the mechanical upper crust is more or less quartz controlled (Brace & Kohlstedt 1980), the mechanical behaviour of the lower and middle crust may be conditioned by a variety of lithologies such as quartz diorite, diabase, plagioclase. The major difference between the mechanical properties of these minerals and those of the mantle rocks is that the crustal materials normally have much lower temperatures of creep activation. If the crust is thick [>35 km (Burov & Diament 1995)], the lower crustal temperatures may be high enough to result in negligible creep strength of the rocks in the vicinity of the Moho. This effect may lead to mechanical decoupling between the crustal and mantle lithospheres (e.g. Meissner & Wever 1988; Kusznir & Matthews 1988; Lobkovsky 1988; Lobkovsky & Kerchman 1992). At the same time, the mechanical properties of the different crustal rocks also differ significantly from each other. For example, quartz-controlled rocks begin to flow at temperatures of a few hundreds degrees below those inferred for diabase. Such temperature differences correspond to a depth interval of a few tens of kilometres. Therefore, depending on the rheological composition, segments of continental crust with the same thickness may have quite different mechanical strengths. This problem is somewhat complicated

Figure 1. Location map of EET data points superimposed on the free-air (FAA) gravity anomaly map. The FAA gravity data converted to Bouguer anomalies are a major source for the estimation of the EET values. The data set presented here is based on R. Rapp's $30' \times 30'$ and $60' \times 60'$ catalogues (Rapp & Pavlis 1990; GEODAS CD-ROM 1992), improved by incorporation of the European gravity data from GEODAS CD-ROM (1992), and has parts re-digitized from various published Russian gravity data [$60' \times 60'$ data for the area between 6°E–165°W and 30–75°N (Artemjev *et al.* 1994), and pieces of $60' \times 60'$ and $5' \times 7.5'$ data (e.g. Burov *et al.* 1990, 1993, 1994; Artemjev *et al.* 1992a,b, 1994; Artemjev & Kaban 1994)] and Chinese gravity data (Ma 1987a,b). The numbers on the map refer to EET estimates (km) given in this paper for the areas investigated here. The political boundaries are kept as they were in 1990.

Notation used:

NBS.–Northern Baltic Shield (Cloetingh & Banda 1992).
CBS.–Central Baltic Shield (Cloetingh & Banda 1992).
SBS.–Southern Baltic Shield (Cloetingh & Banda 1992).
FE–Fennoscandia (Morner 1990).
EIFEL–Eifel, Variscan of central Europe (Cloetingh & Banda 1992).
NHD–North Hessian Depression, Variscan of central Europe (Cloetingh & Banda 1992).
URA–Urach, Variscan of central Europe (Cloetingh & Banda 1992).
JURA–Jura, Alpine EGT (Cloetingh & Banda 1992).
MOLL–Molasse basin, Alpine EGT (Cloetingh & Banda 1992).
AAR–Aar-Gotthard, Alpine EGT (Cloetingh & Banda 1992).
S.A.–Southern Alps (Royden 1993; Okaya *et al.* 1996; Bertotti *et al.* 1996).
E.A.–Eastern Alps (Royden 1993; Okaya *et al.* 1996; Bertotti *et al.* 1996).
CS–Carpathians (Royden 1993; McNutt & Kogan 1987; Zoetemeijer *et al.* 1994; Matencu *et al.* 1994).
CA–Caucasus (Russian plate side) (Ruppel 1992; Stakhovskaya & Kogan 1993).
UR–Urals (Russian plate) (Kruse & McNutt 1988; McNutt & Kogan 1987; Stakhovskaya & Kogan 1993).
NB–North Baikal (Burov *et al.* 1994).
VE–Verkhoyansk plate (McNutt *et al.* 1988).
DZ–Dzungarian basin, Central Asia (Benedetti 1993).
TA–Tarim plate, south (Lyon-Caen & Molnar 1984); centre and north (Burov *et al.* 1990).
Ebro–Ebro Basin (Zoetemeijer *et al.* 1990).
Betic M.–Betic rift margin (Peper & Cloetingh 1992).
Cord.–Betic Cordilleras (van der Beek & Cloetingh 1992; Cloetingh *et al.* 1992).

EET data location map and FAA map (base: R.Rapp 30'x30' & 60'x60'; Artemjev et al., 1994)

Compilation from multiple sources

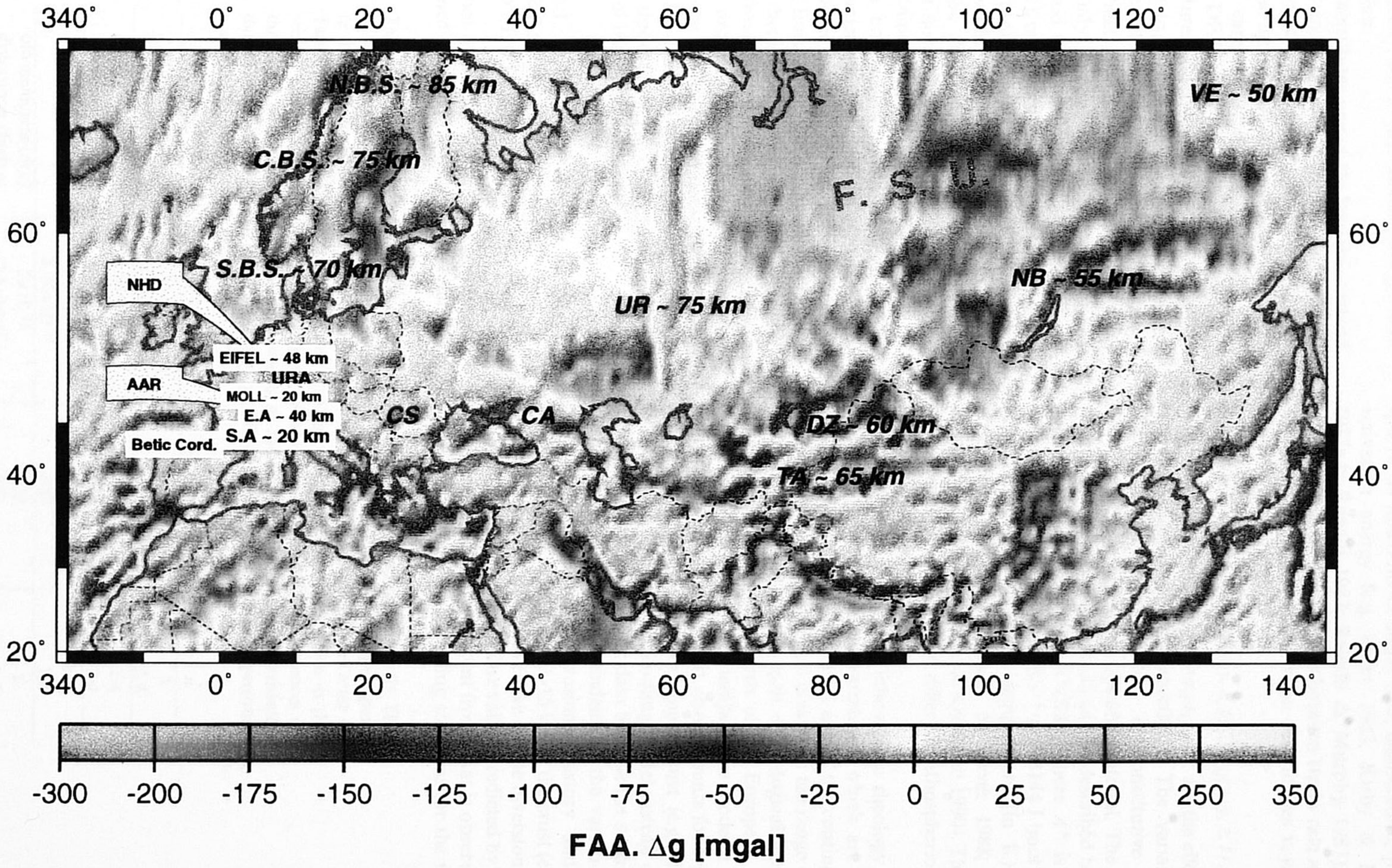

by the fact that the elastic parameters of different crustal rocks do not differ as much as their ductile properties do. Consequently, when the stress is below the yielding limits, the crust behaves quasi-elastically, and its mechanical strength does not depend on composition.

Europe's lithosphere constitutes one of the best investigated areas in the world, and an extensive amount of high-quality geophysical data is nowadays available to constrain thermo-mechanical models of the lithosphere. Deep seismic reflection and refraction surveys carried out by European scientific consortia (e.g. BIRPS, DEKORP, EGT, ECORS, BABEL) have revealed deep structures underlying different age segments of Europe's lithosphere (e.g. Blundell, Freeman & Mueller 1992; Meissner & Bortfeld 1990; Roure, Heitzmann & Polino 1990; Bois, Gabriel & Pinet 1990; Balling 1992; Klemperer & Hobbs 1991). For this study, we chose a set of recently studied localities from and around the European Geotraverse (Fig. 1; Cloetingh & Banda 1992), covering almost the whole spectrum of thermo-tectonic ages presented in the Eurasian lithosphere, varying from Precambrian Scandinavian lithosphere to young Alpine orogenic belts. We also completed our data set with several new data points now available from eastern Europe and the former Soviet Union (FSU) (Fig. 1).

We will begin with a brief review of the rock mechanics constraints on the mechanical properties of the lithosphere, on the basis of which we subsequently construct strength profiles for different segments of Europe and Eurasia. This is followed by a comparison of the rheologically predicted EET estimates with EET data obtained from flexural studies for a large number of basins, forelands and orogenic belts. We also examine the role of the intra-plate stresses as a factor in contributing to the observed differences in EET estimates, and discuss the relationships between the EET, thickness of the competent crust and mantle and wavelengths of lithospheric folding.

2 EXPERIMENTAL DATA ON THE MECHANICAL PROPERTIES OF THE LITHOSPHERE: OVERVIEW

The finite-strain properties of the lithosphere and underlying asthenosphere are governed by empirical constitutive relations that express the yield stress limits of quartz (upper crust), diabase, quartz diorite, plagioclase (lower crust) and olivine (mantle), the dominant lithologies within the continental lithosphere, as functions of strain rate, temperature, pressure and activation energy (e.g. Kirby 1983; Kirby & Kronenberg 1987a,b; Ranalli 1987; Ranalli & Murphy 1987). In a generalized form the relationship between strain rate and stress at a point $\{x, y, z, t\}$ with Cartesian coordinates x, y, z at time t is given by

$$\dot{\varepsilon}_{ij}(x, y, z, t) = D(x, y, z, t)\sigma(x, y, z, t)^{n-1}\sigma_{ij}(x, y, z, t), \qquad (2.1)$$

where $\dot{\varepsilon} = (\dot{e}_{ij}\dot{\varepsilon}_{ij}/2)^{1/2}$ and $\sigma = (\sigma_{ij}\sigma_{ij}/2)^{1/2}$ are the effective strain rate and effective stress, respectively. The variables n (the effective stress exponent) and D (constitutive parameter) describe the properties of a specific material. The dislocation creep of most lithospheric rocks can be described by (2.1) with $n = 3$–5 and $D = A^* \exp(-H^*/RT)$, where A^* is a material constant, $R = 1.986$ cal (mol K)$^{-1}$ or 8.3144 J (mol K)$^{-1}$ is the gas constant and T is the temperature (in K) (Kirby & Kronenberg 1987a,b; Meissner & Wever 1988; Ranalli & Murphy 1987; Mackwell, Bai & Kohlstedt 1990). The commonest material parameters for different lithospheric rocks and minerals are given in Table 1.

As mentioned above, the lithospheric rheology is strongly controlled by temperature variations, which are themselves directly related to the geological age of the continental plates (e.g. Sclater *et al.* 1981). Fig. 2 illustrates the range of temperatures characteristic for the span of geological age variations representative for the segments of the European lithosphere discussed in this paper. This temperature model is based on a semi-space cooling model that also accounts for typical radiogenic heat generation in the upper crust (e.g. Burov *et al.* 1993). We prefer to use the cooling model instead of inversion (integration) of the heat flux data because the surface heat flux in the continents is too dependent on the variations in heat production, sedimentation/erosional history and structural inhomogeneities in the first 10–15 km of the crust (e.g. England & Richardson 1980). However, we do use inversion of the heat flux in the areas where heat flux values predicted by the cooling model are significantly different from what is observed. In such areas, we combine plate-cooling solutions for the mantle part

Table 1. Parameters of dislocation creep for major lithospheric rocks and minerals. The data sources (values given in the first lines of the table for each rock/mineral) adopted in the paper for construction of the strength profiles (Brace & Kohlstedt 1980; Carter & Tsenn 1987; Tsenn & Carter 1987; Kirby & Kronenberg 1987a,b). The values in the second lines are from data sources that have been used to explore the consequences of the range of uncertainties intrinsically related to the extrapolation of rock mechanics data (Fig. 5b) (Ranalli 1987; Ranalli & Murphy 1987; Ranalli 1995, Ranalli 1995, personal communication).

Mineral/rock	A^* [Pa^{-n} s^{-1}]	H^* [kJ mol^{-1}]	n
quarzite (dry)	5×10^{-12}	190	3
	2.7×10^{-20}	156	2.4
diorite (dry)	5.01×10^{-15}	212	2.4
	5.2×10^{-18}	219	2.4
diabase (dry)	6.31×10^{-20}	276	3.05
	8.00×10^{-25}	260	3.4
olivine/dunite (dry) dislocation climb at $\sigma_1-\sigma_3 \le 200$ MPa	7×10^{-14}	520	3
	2.5×10^{-17}	532	3.5
olivine (Dorn's dislocation glide) at $\sigma_1-\sigma_3 \ge 200$ MPa)	$\dot{\varepsilon} = \dot{\varepsilon}_0 \exp\left[-H^*\left(1-(\sigma_1-\sigma_3)/\sigma_0\right)^2/RT\right]$ where $\dot{\varepsilon}_0 = 5.7\times10^{11}$ s^{-1}, $\sigma_0 = 8.5\times10^3$ MPa; $H^* = 535$ kJ mol^{-1}		

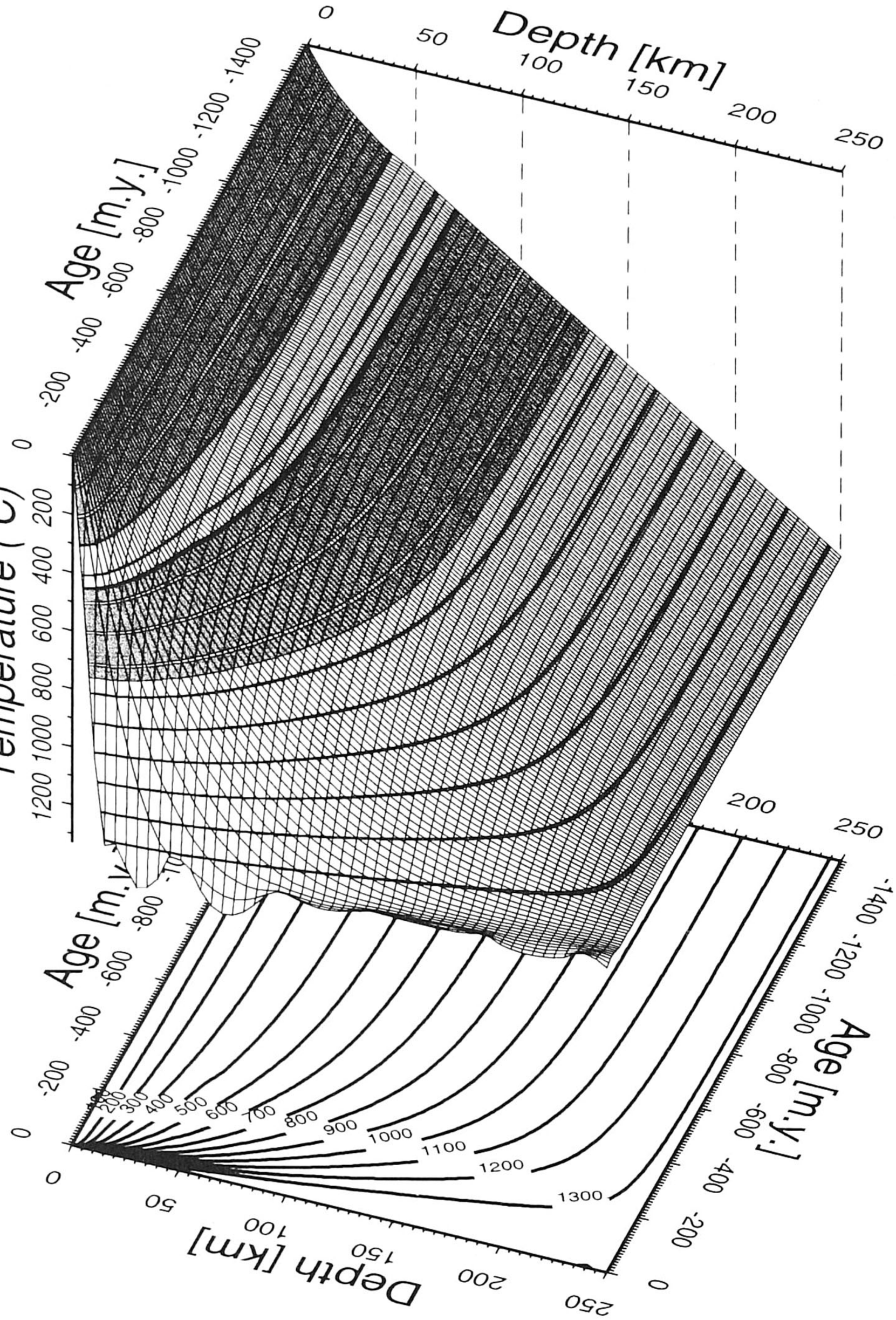

Figure 2. Thermal model of the continental lithosphere based on a semi-space cooling model and accounting for typical radiogenic heat production in the upper crust (e.g. after Burov *et al.* 1993). The equilibrium thermal thickness of the lithosphere is 250 km. The parameters of the thermoconductivity equations used here are $\rho_c = 2650\ \mathrm{kg\ m^{-3}}$, $\rho_{c2} = 2900\ \mathrm{kg\ m^{-3}}$; $k_c = 2.5\ \mathrm{W\ m^{-1}\ K^{-1}}$; $k_{c2} = 2\ \mathrm{W\ m^{-1}\ K^{-1}}$; $k_m = 3.5\ \mathrm{W\ m^{-1}\ K^{-1}}$; $\chi_c = 8.3 \times 10^{-7}\ \mathrm{m^2\ s^{-1}}$; $\chi_{c2} = 6.7 \times 10^{-7}\ \mathrm{m^2\ s^{-1}}$; $\chi_m = 8.75 \times 10^{-7}\ \mathrm{m^2\ s^{-1}}$; $H_s = 7.5\text{–}9.5 \times 10^{-10}\ \mathrm{W\ kg^{-1}}$; $H_{c2}C_{c2}^{-1} = 1.7 \times 10^{-13}\ \mathrm{K\ s^{-1}}$. Here, $\chi_{c1}, \chi_{c2}, \chi_m$ are coefficients of the thermal diffusivity, and k_{c1}, k_{c2} and k_m are the respective coefficients of thermal conductivity of the upper crust, lower crust and mantle; t is time; ρ_c, ρ_{c2} are the densities of the upper and lower crust, respectively; H_s is the surface radiogenic heat production rate per unit mass; and $h_r \approx 10$ km is the depth scale for the decrease in radiogenic heat production. The numbers in the lower panel are temperatures in degrees (°C) for isotherms plotted at 100 °C intervals.

of the lithosphere with the solutions obtained by heat flux inversion for the crust.

The brittle properties of the rocks depend on pressure, but not on temperature or rock type (Byerlee 1978):

$$\begin{cases} \sigma_3 = (\sigma_1 - \sigma_3)/3.9 & \text{for } \sigma_3 < 120\ \mathrm{MPa}, \\ \sigma_3 = (\sigma_1 - \sigma_3)/2.1 - 100 & \text{for } \sigma_3 \geq 120\ \mathrm{MPa}, \end{cases} \tag{2.2}$$

where $\sigma_1, \sigma_2, \sigma_3$ are the principal stresses.

In terms of the principal stresses, the elastic, or quasi-elastic, behaviour can be described by the linear stress–strain relation

$$\sigma_j = 2\mu\varepsilon_j + \lambda(\varepsilon_1 + \varepsilon_2 + \varepsilon_3) \quad \text{where } j = 1, 2, 3. \tag{2.3}$$

λ and μ are Lamé's constants related to Young's modulus (E) and Poissons's ratio v as $\lambda = Ev[(1+v)(1-2v)]^{-1}$; $\mu = E/2(1+v)$. Typically inferred values for E and v are $6.5 \sim 8 \times 10^{10}$ N m^{-2} and 0.25, respectively (e.g. Watts 1978; Turcotte & Schubert 1982). Although the elastic properties change with depth, these changes are relatively unimportant compared with the changes in other properties of the lithospheric materials.

By combining rheological laws, the eqs (2.1)–(2.3) form piecewise continuous yield-stress envelopes (see Fig. 3). The

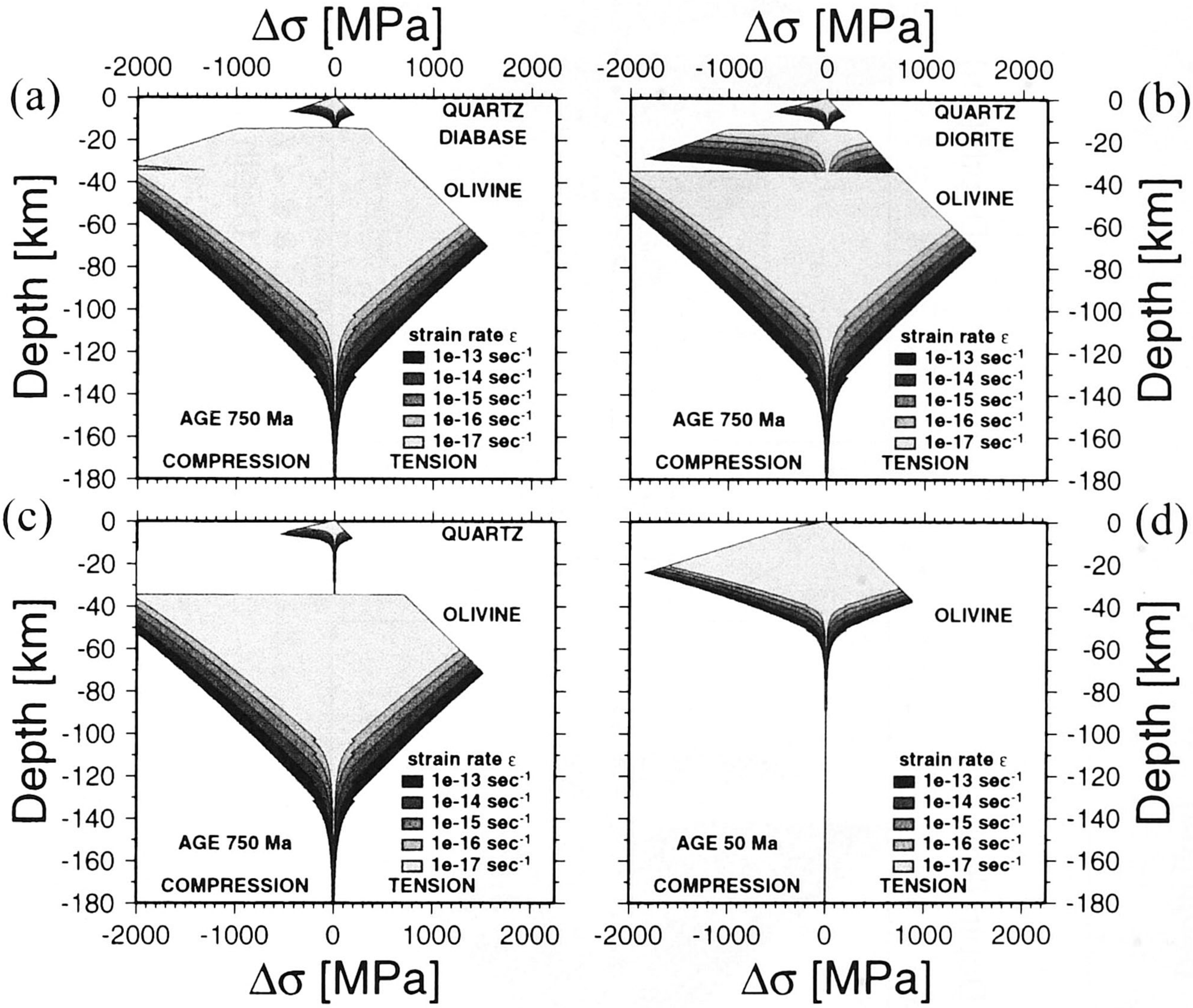

Figure 3. Yield-strength envelopes (YSE) calculated by extrapolation of rock mechanics data. Different panels illustrate the effects of variations in the mineral composition of the crust and of the basic strain rate adopting an age of 750 Ma for the continental lithosphere and 50 Ma for the oceanic lithosphere. Dependent on the adopted rheology, mechanical decoupling zones may appear on different levels of the crust. The variation of the strain rate is relatively unimportant for the mechanical structure of the lithosphere. See Table 1 for the rheological parameters adopted in the construction of the strength profiles.

Figure 4. Effect of the flexural stresses and horizontal force on the effective strength of the lithosphere. YSE is calculated for a typical strain rate of 3.5×10^{-15} s^{-1}. (a) Effect of the extensional horizontal force (stress levels of 100, 200, 500 MPa marked by different shadings) on weakening of the lithosphere. Where the stress reaches the yield strength, the lithosphere undergoes inelastic deformation (brittle or ductile) and becomes weak. (b) Effect of the bending stresses (moderate plate curvature and basic strain rate of 3.5×10^{-15} s^{-1}) and the presence of an extensional horizontal tectonic force leading to stress amplification and attenuation. Thick dashed lines schematically show the geometry of the surfaces of the down-bent plate. The vertical arrow marks the position of the vertical load operating on the lithosphere. Dashed lines correspond to strain rates of $\dot{\varepsilon} = 10^{-13}; 10^{-14}; 10^{-15}; 10^{-16}; 10^{-17}$ s^{-1}. Note the interruptions in stress distributions at the sides of intra-lithospheric decoupling zones.

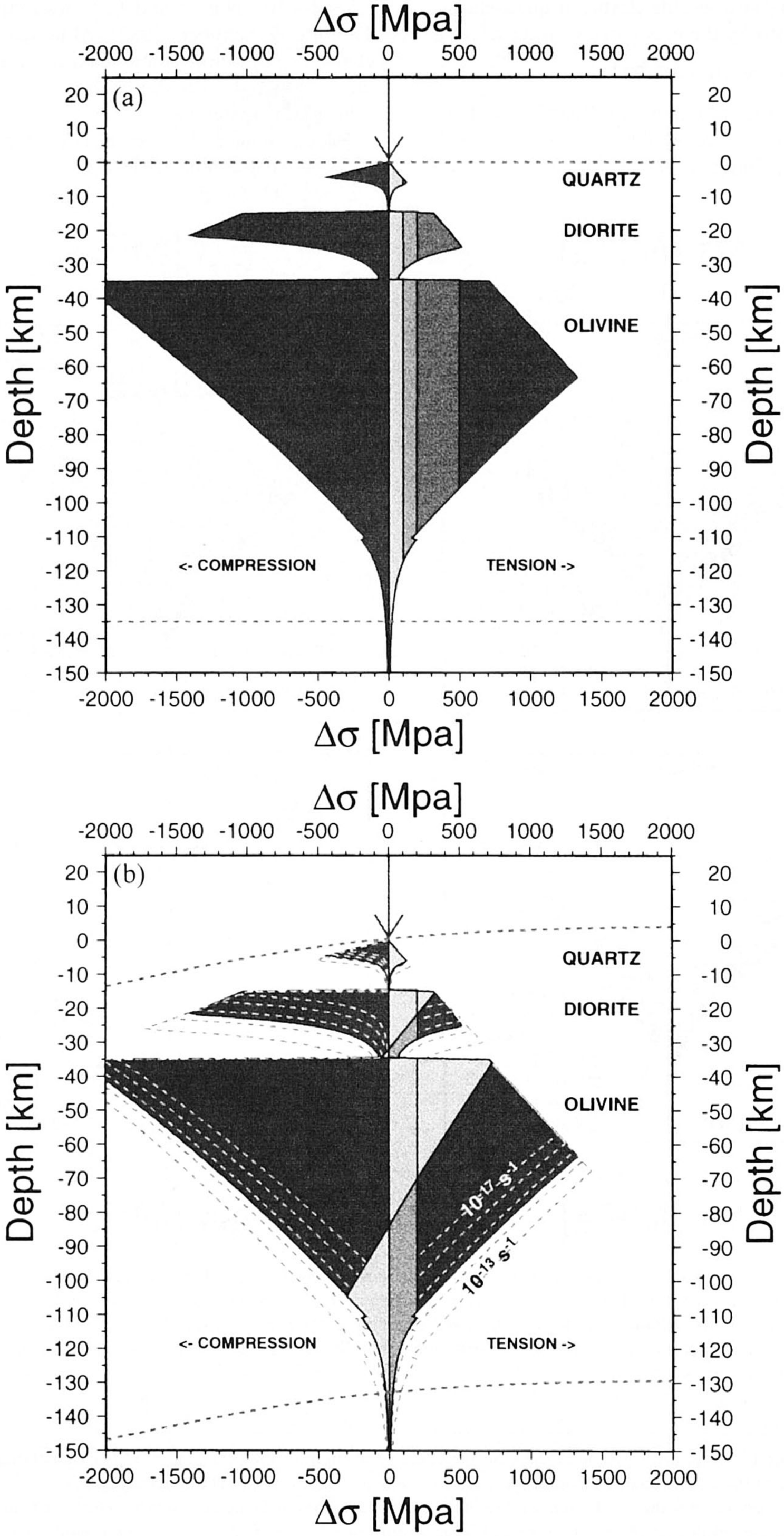
Δσ [Mpa]
-2000 -1500 -1000 -500 0 500 1000 1500 2000
(a)
QUARTZ
DIORITE
OLIVINE
<- COMPRESSION
TENSION ->
Depth [km]
20 10 0 -10 -20 -30 -40 -50 -60 -70 -80 -90 -100 -110 -120 -130 -140 -150
Δσ [Mpa]
Δσ [Mpa]
(b)
QUARTZ
DIORITE
OLIVINE
10-17 s-1
10-13 s-1
<- COMPRESSION
TENSION ->
Depth [km]
Δσ [Mpa]

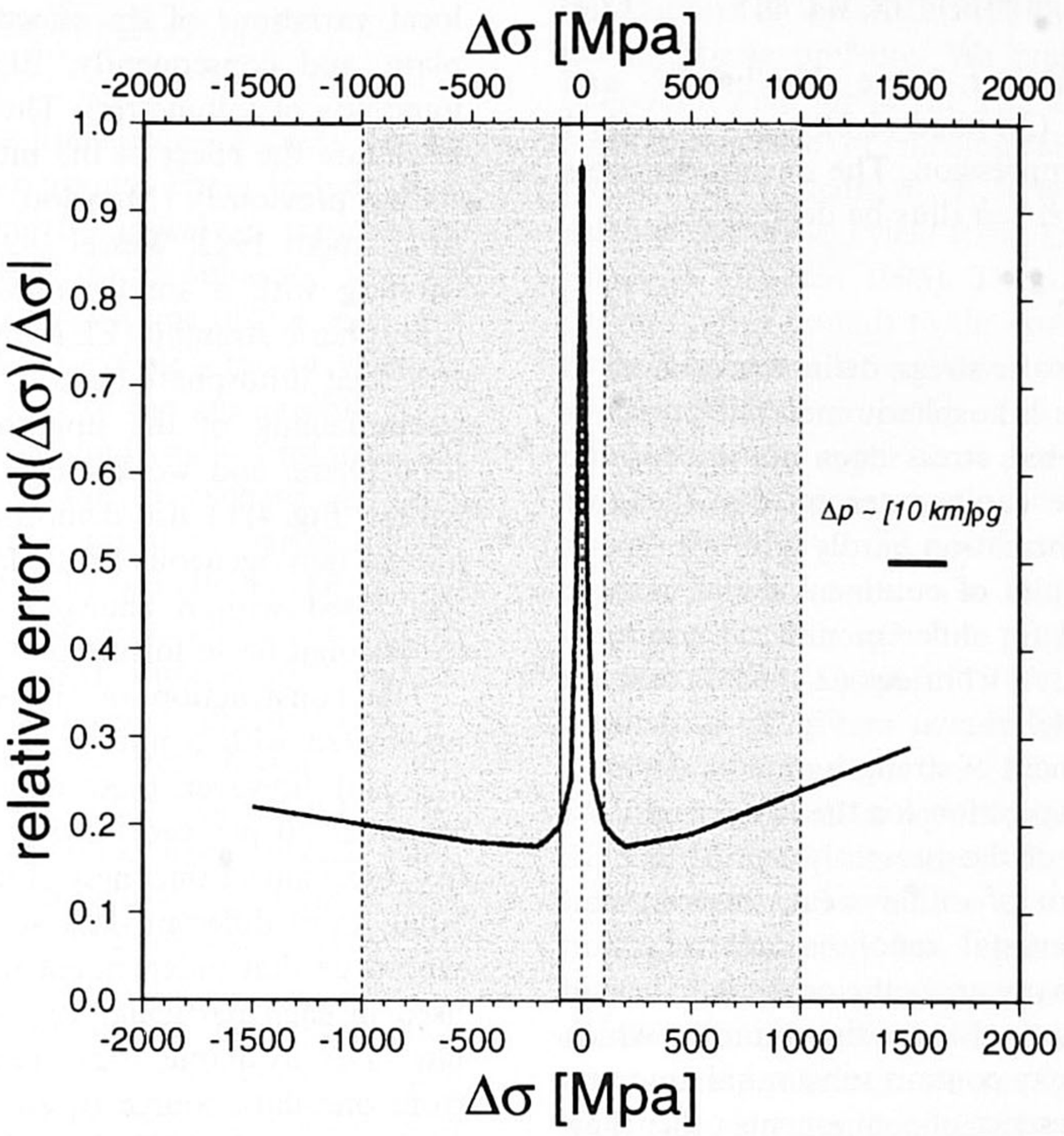

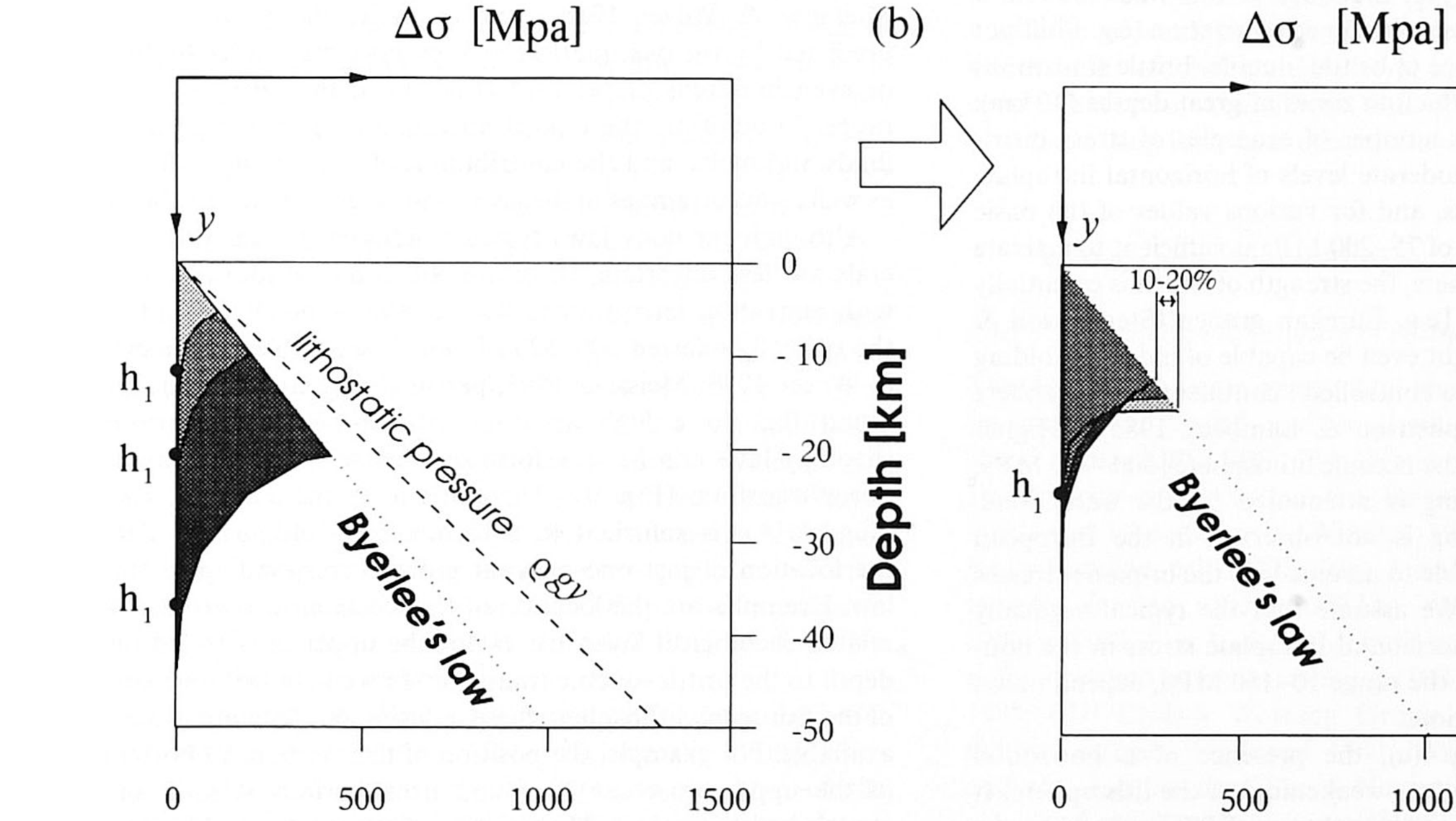

Figure 5. (a) Example of typical uncertainties associated with prediction of the mantle rheological structure of the lithosphere, assuming that Moho depth and depth to the mechanical bottom of the lithosphere are known from independent data. This example refers to the Precambrian lithosphere of the Baltic shield (see Fig. 6a). The grey areas correspond to stress intervals of geological relevance bounded by an upper limit of 1 GPa and by a lower limit of negligible stresses (where the uncertainty is the highest). For the mantle lithosphere, the negligible stress (few per cent of lithostatic pressure) is of the order of several tens of MPa. The length of the small horizontal bar corresponds to the pressure change induced by a 10 km change in depth. Inspection of the figure demonstrates that the 'negligible' stress range corresponds to a few km variation in depth. For the upper-crustal parts, the absolute values of maximum and minimum relevant stresses are 2–3 times lower. The uncertainties (on the assumption that only the positions of the mechanical bottoms of the crustal layers are known) are thus higher. However, more independent observations allow better constraints on the crustal rheology (see text). (b) Example of reduction of the uncertainties in the quartzite rheology. Left: light and medium grey filled areas represent the quartzite creep law from Kirby & Kronenburg (1987a,b; Table 1) calculated for 'hot'

yield-stress envelope can be defined as a contour $\sigma^f = \sigma^f(x, y, t, \dot{\varepsilon})$ such that:

$$\sigma^f = \text{sign}(\varepsilon)\min\{|\sigma^b(x, y, t, \dot{\varepsilon}, \text{sign}(\varepsilon))|, |\sigma^d(x, y, t, \dot{\varepsilon})|\}, \quad (2.4)$$

where $\sigma^b(x, y, t, \dot{\varepsilon}, \text{sign}(\varepsilon))$, $\sigma^d(x, t, t, \dot{\varepsilon})$ are the 'brittle'- and 'ductile'-yielding stresses from (2.1) and (2.2); sign(ε) equals 1 for extension and -1 for compression. The deviatoric stress $\sigma(\varepsilon)$ for the strain $\varepsilon = \varepsilon(x, y, t, \dot{\varepsilon})$ can thus be defined as

$$\sigma(\varepsilon) = \text{sign}(\varepsilon)\min\{|\sigma^f|, |\sigma^e(\varepsilon)|\}, \quad (2.5)$$

where $\sigma^e(\varepsilon)$ is the elastic deviatoric stress, defined according to (2.3). Eq. (2.5) means that the lithospheric material preserves elastic properties if the imposed stress does not exceed the yield strength. The elastic 'core' can be interpreted as the layer in which creep and brittle deformation hardly alter the stress.

Fig. 3 provides some examples of continental and oceanic yield-strength profiles derived for different mineral compositions and strain rates, calculated from eqs (2.1)–(2.5) and on the basis of the thermal model shown in Fig. 2. As demonstrated by Fig. 3, the development of strength minima depends primarily on the adopted composition for the lower crust. As will be discussed later, most of the presently available EET estimates support the presence of rather weak lower-crustal rheologies. Studies of lower-crustal xenoliths and reflection seismic data indicate that in many areas the orogenic fabric of the lower crust is truncated by the Moho discontinuity, which suggests that the lower crust may contain substantial amounts of felsic rocks, implying the presence of components other than mafic granulites (see Ziegler, Cloetingh & van Wees 1995 for a discussion). Also, recent studies on eclogitization (e.g. Phillipot 1993) suggest the presence of brittle–ductile–brittle transitions in the palaeo-alpine subduction zones at great depths (40 km). Figs 4(a) and (b) give a number of examples of stress distributions computed for moderate levels of horizontal intraplate stress and bending stress, and for various values of the basic strain rate. A stress level of 75–200 MPa is sufficient to activate folding of young lithosphere, the strength of which is essentially controlled by the crust [e.g. Eurekan graben (Stephenson & Cloetingh 1991)]. It might even be capable of inducing folding in much older mantle-controlled continental lithosphere [Central Australia (Stephenson & Lambeck 1985)]. Higher stresses are required for the oceanic lithosphere (500–700 MPa; Zuber 1987) since folding is attenuated by the water load. Since lithospheric folding is not observed in the European lithosphere, it is reasonable to assume that the in-plane stresses there are not so high. We assume that the typical vertically averaged values of the horizontal intraplate stress in the non-folded lithosphere are in the range 10–150 MPa, depending on the age and local conditions.

As illustrated in Fig. 4(a), the presence of a horizontal intraplate stress leads to 'pre-weakening' of the lithosphere. It limits the maximum possible value of EET, and shifts the positions of the internal neutral (stress-free) surfaces during plate flexure. The horizontal stress becomes especially important if the condition of a constant tectonic force (Kusznir 1991) is assumed. As illustrated in Fig. 4(b), the plate flexure controls local variations of the effective mechanical thickness of the plate, and consequently, EET on horizontal scales (up to hundreds of kilometres). The bending stress may amplify or attenuate the effect of the intraplate horizontal stress. It was shown previously (McAdoo, Martin & Polouse 1985; Burov & Diament 1992; Wessel 1993; Burov & Diament 1995) that bending with a small radius of flexure can locally reduce lithospheric strength (EET) by a factor of 2–3. Bending of the stretched lithosphere beneath sedimentary basins may lead to strengthening of the uppermost subcrustal portion of the lithosphere, and weakening of the lowermost (mantle) lithosphere. Fig. 4(b) also demonstrates the possible occurrence of almost homogeneous brittle failure in the crust, which may be associated with a change in the depth of necking during extensional basin formation.

The construction of the strength profiles is intrinsically associated with a number of uncertainties. As illustrated by Fig. 5(a), however, these uncertainties may be constrained to maximal 20 per cent, provided some additional information (e.g. mechanical thickness of the competent layers) is available. Analysis of different data sources (Table 1, Fig. 5b) has convinced us that independent information on rheology must be used in each particular case to constrain a specific rheology law. The available rock mechanics data differ significantly from one data source to another (e.g. Kirby & Kronenburg 1987a,b; Ranalli 1987; Ranalli & Murphy 1987; Ranalli 1995; Meissner & Wever 1988). For example, the yield stresses predicted by various quartz rheology laws may differ by tens or even hundreds of per cent (Fig. 5b) in the relevant stress range. In addition, the typical uncertainties in the content of fluids and melts, and the contribution of other mineral facies, as well as uncertainties in the geotherm, aggravate the problem.

Although rheology laws typically adopted for mantle minerals are less uncertain, there are still some peridotite values with activation energy from 400 to 450 kJ mol^{-1} instead of the typically inferred 500–520 kJ mol^{-1} (see Table 1; Meissner & Wever 1988; Meissner 1995, personal communication). We found that to a high accuracy (10–20 per cent), various rheology laws can be transformed to each other by a simple linear transform (Fig. 5b). Therefore, to define a specific rheology law it is sufficient to constrain from *independent data* the location of just one relevant point corresponding to this law. Examples are the location of the mechanical bottom of a related rheological layer (e.g. h_1 for the upper crust), and the depth to the brittle–ductile transition. In well-studied segments of the European lithosphere these independent data are usually available. For example, the position of the mechanical bottom of the upper crust can be found from various seismic and electric resistivity data. The position of the mechanical bottom of the mantle lithosphere can be estimated from seismic data

(radiogenic heat included) and 'cold' upper-crustal geotherms (500 Ma lithosphere). The dark grey area corresponds to parameters proposed by G. Ranalli (1995, personal communication, Table 1). The heat generation in the upper 10 km of the crust is not important in this case. Letters h_1 mark the positions of the mechanical bottom of the upper crust *predicted* by these three rheology laws. Right: if the position of the mechanical bottom of the upper crust (h_1) is known *a priori* from independent observations, all three laws from the left side can be transformed to each other within an accuracy of 10–20 per cent.

and from estimates of the effective elastic thickness of the lithosphere (see next section for more details).

3 STRENGTH PROFILES THROUGH EUROPE AND EURASIA

The mechanical properties of the lithosphere interiors can be deduced from a variety of observations. These include P–T data at different depths in the Earth, laboratory experiments on the mechanical properties of the rocks subjected to such P–T conditions (see Section 2), observations of the geometry of plate bending (allowing extraction of flexural, or effective elastic parameters and the thickness of the mechanical lithosphere), and data on postglacial rebound yielding information on the visco-elastic properties of the lithosphere. Another source of information on the mechanical properties of the lithospheric interiors is from xenoliths brought to the surface from various depths by volcanic processes. The eclogitization data provide considerable direct information on deformation regimes of the deep rocks, such as crack sealing, and ductile–brittle–ductile transitions observed at great depths in subduction zones (e.g. Philippot 1987, 1993; Austrheim 1994). Important information can be obtained from seismic data, data on electrical and thermal conductivity, and from data on density distributions (including inversions of gravity and seismic velocity anomalies).

Using the empirical constitutive equations given in Section 2, and geophysical data on crustal and mantle structure, we have constructed a set of yield-strength profiles for various sites along the European Geotraverse, as well as for a number of other localities in Eurasia. The European lithosphere is one of the best-studied areas on Earth, and a synthesis of all present-day available data is carried out for the investigation of the thermomechanical structure of these geographically large segments of the world's continental lithosphere. Our study also covers a number of regions in eastern Europe and the FSU. The data used include various types of seismic data (seismicity–depth patterns, seismic refraction and reflection profiles, reflectivity data, attenuation of seismic waves), petrological and geological data, magnetotelluric (M–T)/electric resistivity measurements, heat flow, xenolith and gravity data. For example, clear indications for the crust–mantle decoupling and constraints on the thickness of the upper and lower crust can be found from the seismic reflectivity (lamellae) data (Wever 1989; Beaumont & Quinlan 1994; Marquis, Jones & Hyndman 1995). Such data for Europe suggest decoupling for >75 per cent of the European crust (Meissner 1995, personal communication, BIRPS, DEKORP, EGT, ECORS, BABEL data: see Introduction for the references).

In the strength profiles, we discriminate between the MSC (mechanically strong crust), MSL (mechanically strong lithosphere), and lower values of the depth to the base of the corresponding *competent* layers (h_1, h_2, h_3: upper and lower crusts and mantle lithosphere, respectively). If the lower crust is weak, only two competent layers will be present, crustal and mantle (h_1 and h_2). The values of h_1, h_2, h_3 do not coincide exactly with the values of MSC and MSL. The values for MSC and MSL are traditionally associated with a specific geotherm at which the yield stress is less than some pre-defined low value (e.g. 10–20 MPa used in Ranalli 1994). This definition is not always self-consistent since, for the shallow upper crust, the stress of 10 MPa may be quite high compared with the lithostatic pressure, whereas for the deep mantle lithosphere it is about 0.1 per cent of the lithostatic pressure. It is evident that, even in the absence of strong topographic loads acting on the plate, local fluctuations of the stress field can easily reach 1–5 per cent of the lithostatic pressure. We prefer to use the pressure-scaled minimum yield stress for the definition of the depth to the mechanical base of rheological layers h_1, h_2, h_3. The other possible way to define h_1, h_2, h_3 is to relate them to the minimum value of the vertical yield stress gradient (e.g. 10–15 MPa km^{-1}; Burov & Diament 1995). The values of MSC and MSL thus provide upper bounds to the corresponding values of h_1, h_2, h_3. In the absence of strong lower or middle crust, the sequence of competent layers is restricted to h_1, h_2, where h_1 is the effective thickness of the upper crust and h_2 is the effective thickness of the competent upper mantle. To some extent one can associate h_1 with the EET of the upper crust and h_2 with the EET of the mantle. As will be shown in the next section, the total EET of the decoupled lithosphere is proportional to a cubic root from the sum of the cubes of EETs of the competent crust and mantle. Thus if the lithosphere is very young and the mantle is hot, the mantle contribution to the EET will be minor, and the EET of the lithosphere will be equal to the EET of the crust. In contrast, in the old cold lithosphere the contribution of the crustal strength is much lower than that of the mantle.

Our synthetic yield-strength profiles cover almost all age ranges of the Eurasian lithosphere. They include three points of different ages on the Precambrian Baltic shield, several intermediate points in central Asia, the Russian and Siberian platforms that are dominated by Palaeozoic segments, three points located on the central European Variscan lithosphere, a number of localities in the Jurassic Caucasus, and Miocene Carpathian fold belts, and several sites in the western and central European Alpine belts. Below, we give an abbreviated tectonic setting for most representative profiles.

3.1 Western and Central Europe

3.1.1 Precambrian lithosphere of northern Europe

The European Geotraverse data include three points from the northern, central and southern regions of the Baltic shield (NBS, CBS, SBS, Figs 1 and 6a–6c). The age of the Precambrian rocks within the Baltic shield decreases from north-east to south-west (Windley 1992). The northernmost Kola–Karelian belt (NBS, Figs 1 and 6a) contains Archean terranes formed about 2000 Ma ago. The Sveco–Fennian orogen (CBS, Figs 1 and 6b) is built up with material substantially reworked by crustal melting 1500–1800 Ma ago (Windley 1992; EUGENO-S Working Group 1988). The south-west Gothian orogen developed 1500–1700 Ma ago (SBS, Figs 1 and 6c), and the near Sveco–Norwegian orogen is 1000 Ma old. The Kola–Karelian orogen (NBS) has a crust with distinctively different properties from those of Sveco–Fennian orogen. The crust is on average 45 km thick, with a dominant magnetic dioritic upper layer and an eclogite transition inferred below 38 km (Henkel *et al.* 1990). The Sveco–Fennian orogen (SBS, Figs 1 and 6c) developed by growth and collision of 2000 Ma juvenile arcs and by later crustal melting in 1500–1800 Ma. The upper crust is mainly paramagnetic dioritic with an average crustal thickness of 48 to 54 km (Windley 1992). It is also characterized by a thick lower-crustal layer with a *P*-wave

velocity of 6.8–7.8 km s^{-1} and an eclogite transition at 36 km depth (Henkel *et al.* 1990).

The Gothian orogen (SBS, Figs 1 and 6c) includes areas of acidic metavolcanics (with an age of 1700 Ma), metabasites, quartzites, diorites, mica schists, gneisses, and intrusive granites. The Sveco–Norwegian orogen gave rise 1000 Ma ago to a N–S Cordilleran and collisional belt and later intrusive rocks. Both Gothian and Sveco–Norwegian lithosphere can be characterized by a three-layer crust with a thickness of about 40–45 km.

3.1.2 Variscan lithosphere: Eifel, North Hessian Depression, Urach (Figs 1 and 7)

The Variscan collisional belt formed during the Devonian between 360 and 380 Ma ago (e.g. Franke 1992). This collision was accompanied by high-pressure metamorphism. Plate convergence continued for 100 Myr, and resulted in turning the Variscan belt into an Alpine-type orogen. The thickness of the Variscan crust is remarkably constant, with a value of approximately 30 km. Intraplate seismicity is limited to a depth of 20–30 km, corresponding to isotherms of 450–600 °C. The pre-Permian basement at the localities discussed here along the central segment of the European Geotraverse underwent a complex tectonic evolution of opening and closure of oceanic basins. This ocean was closed during the Silurian, leading to Caledonian deformation of wide areas, including the Tornquist Zone. Variscan basin formation took place to the south of the Iapetus/Tornquist suture as a result of Cambro–Ordovician rifting, whereas the Rhenohercynian basin appears to have been formed during Devonian times (Franke 1992). Closure of these basins was completed in Carboniferous times.

Permo–Carboniferous volcanics required a strong thermal perturbation in the upper mantle after the final closure of the Variscan oceans. As pointed out by Franke (1992), continental subduction during the Variscan collision could have recycled radioactive heat sources into the upper mantle. Excellent constraints on deep crustal structure of Variscan central Europe are available as a result of extensive deep seismic profiling (Meissner & Bortfeld 1990). Despite this, deciphering of the

(a) **Northernmost Baltic Shield (Point FG).**

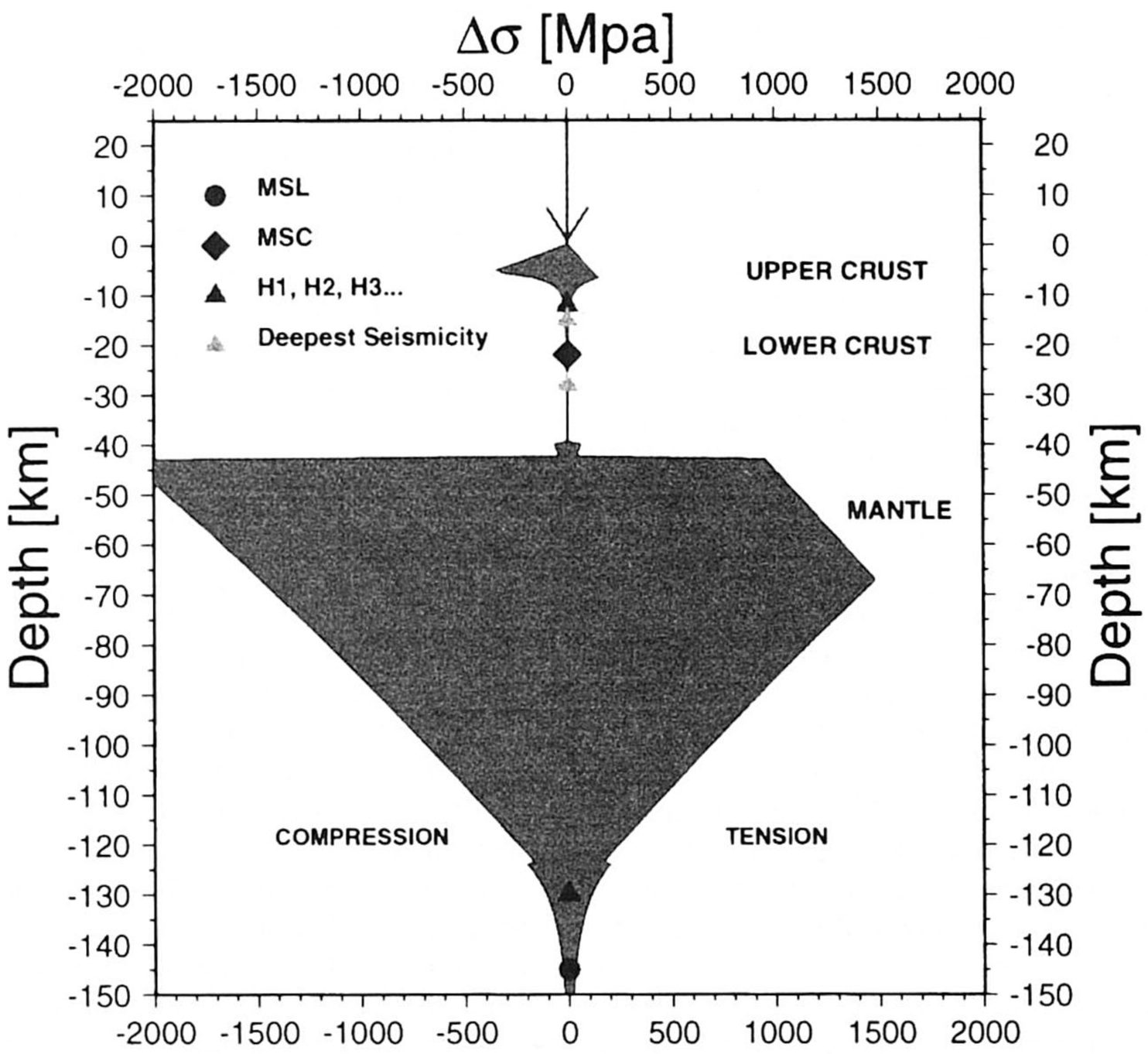

Figure 6. Predicted yield-stress envelopes for the Baltic Shield derived on the basis of heat flux data, age data, petrology and seismic data. Quantities MSC and MSL correspond to the depth to the bottom of the mechanically strong crust, and mechanically strong lithosphere, respectively, defined as a depth to a specific isotherm (see text). Quantities h_1, h_2, h_3 (marked H1, H2, H3 in the figure) represent lower values of the depth to the base of the corresponding competent layers: upper, lower crust and mantle lithosphere, respectively. They are defined as depths at which the yielding strength is below 1–5 per cent of the lithostatic pressure, and the vertical yield-stress gradient is less than 10–15 MPa km. The values of MSC and MSL provide upper bounds to the corresponding values of h_1, h_2, h_3. Circles correspond to MSL estimates; diamonds correspond to MSC estimates; h_1, h_2, h_3 are shown with triangles. According to McNutt *et al.* (1988) and Burov & Diament (1995), the minimum curvature of the lithospheric plates is $<10^{3.5}$ km (radius of the Earth is $\sim 10^{3.7}$ km). This curvature is associated with bending stresses that limit MSC and MSL of the lithosphere. The YSE are calculated for a typical strain rate of 3.5×10^{-15} s^{-1}. (a) northern Baltic shield; (b) central Baltic shield; (c) southern Baltic shield.

(b) **Central Baltic Shield (Point FE).**

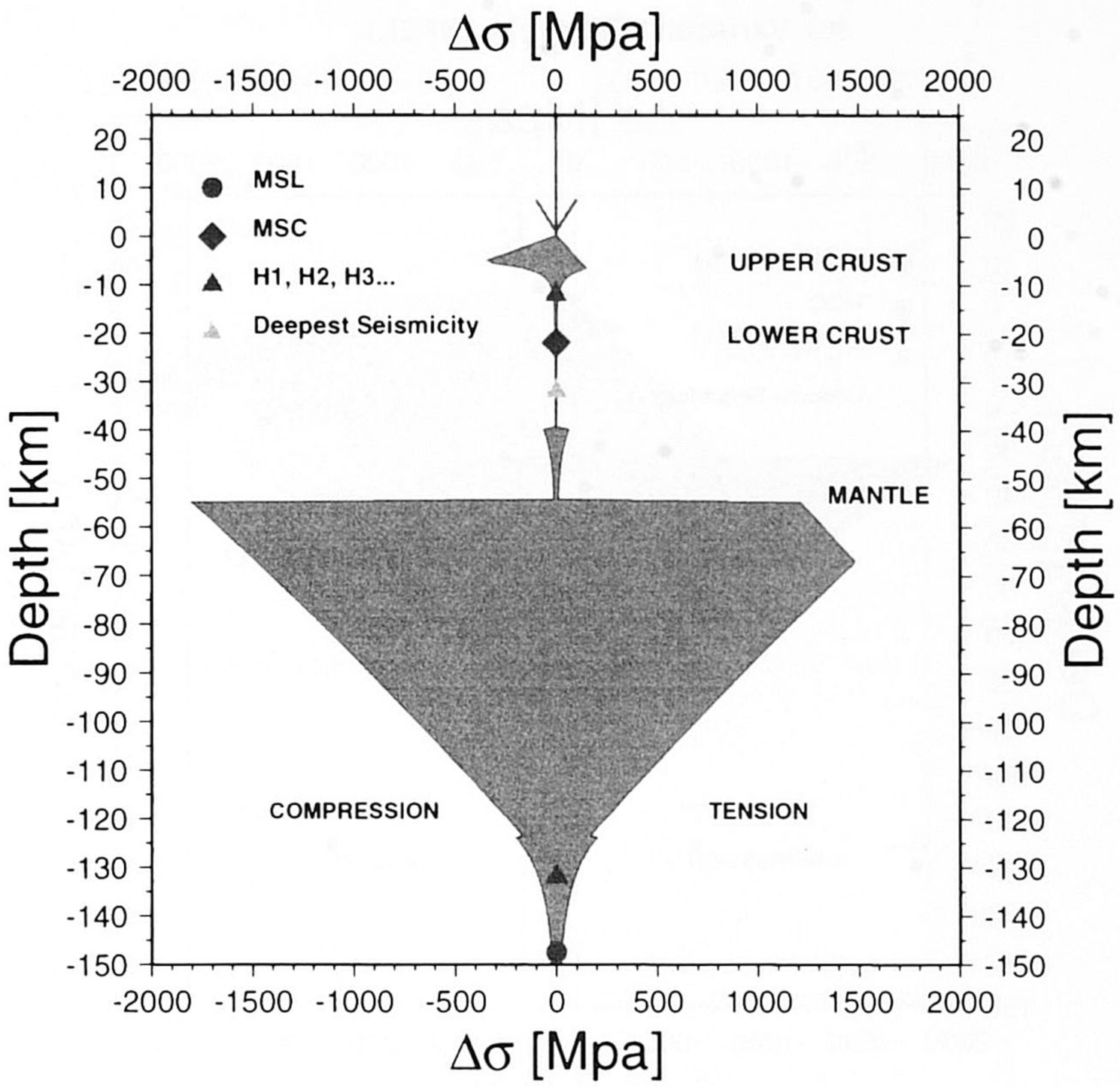

(c) **Southernmost Baltic Shield (Point FC).**

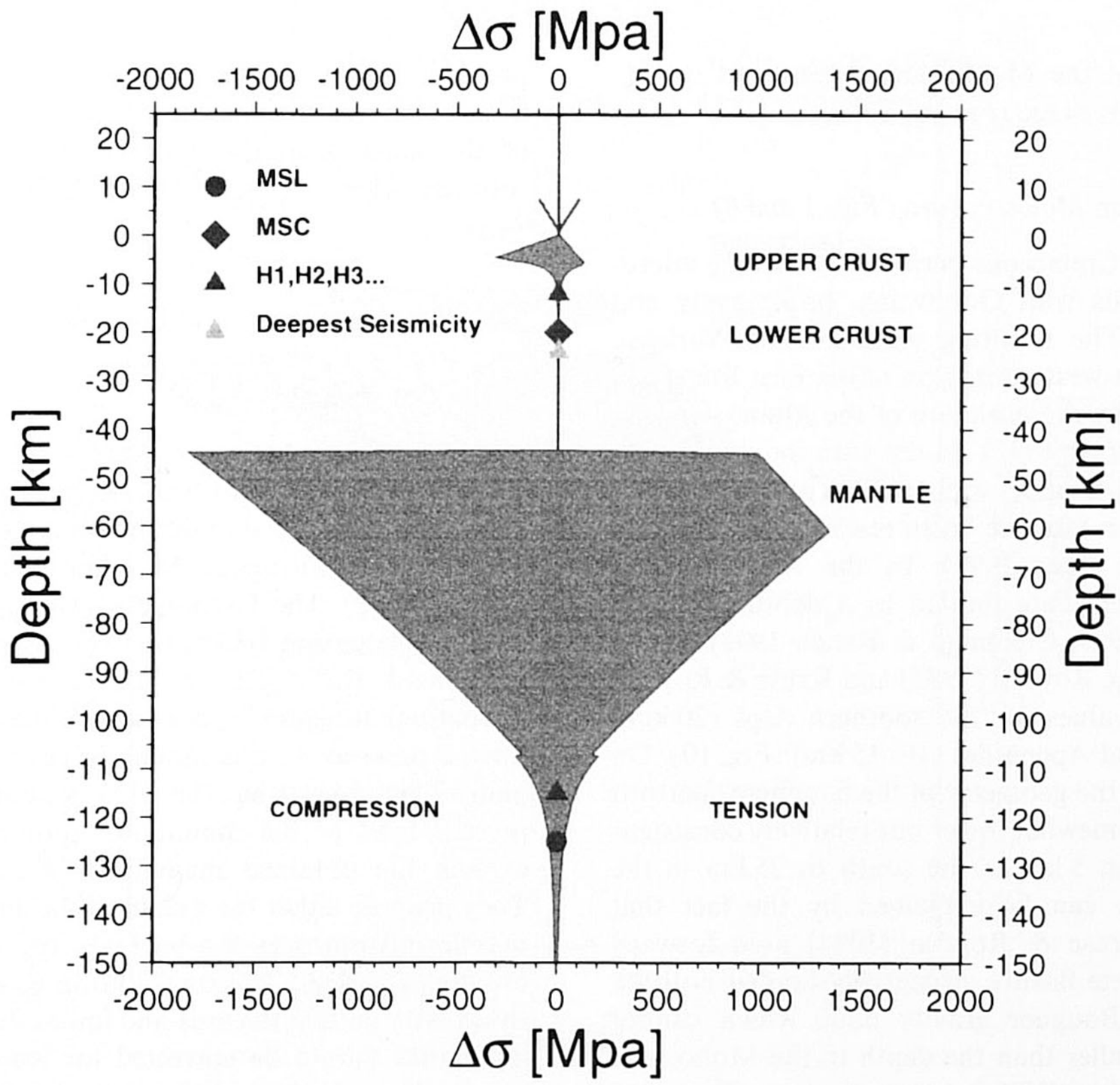

Figure 6. (*Continued.*)

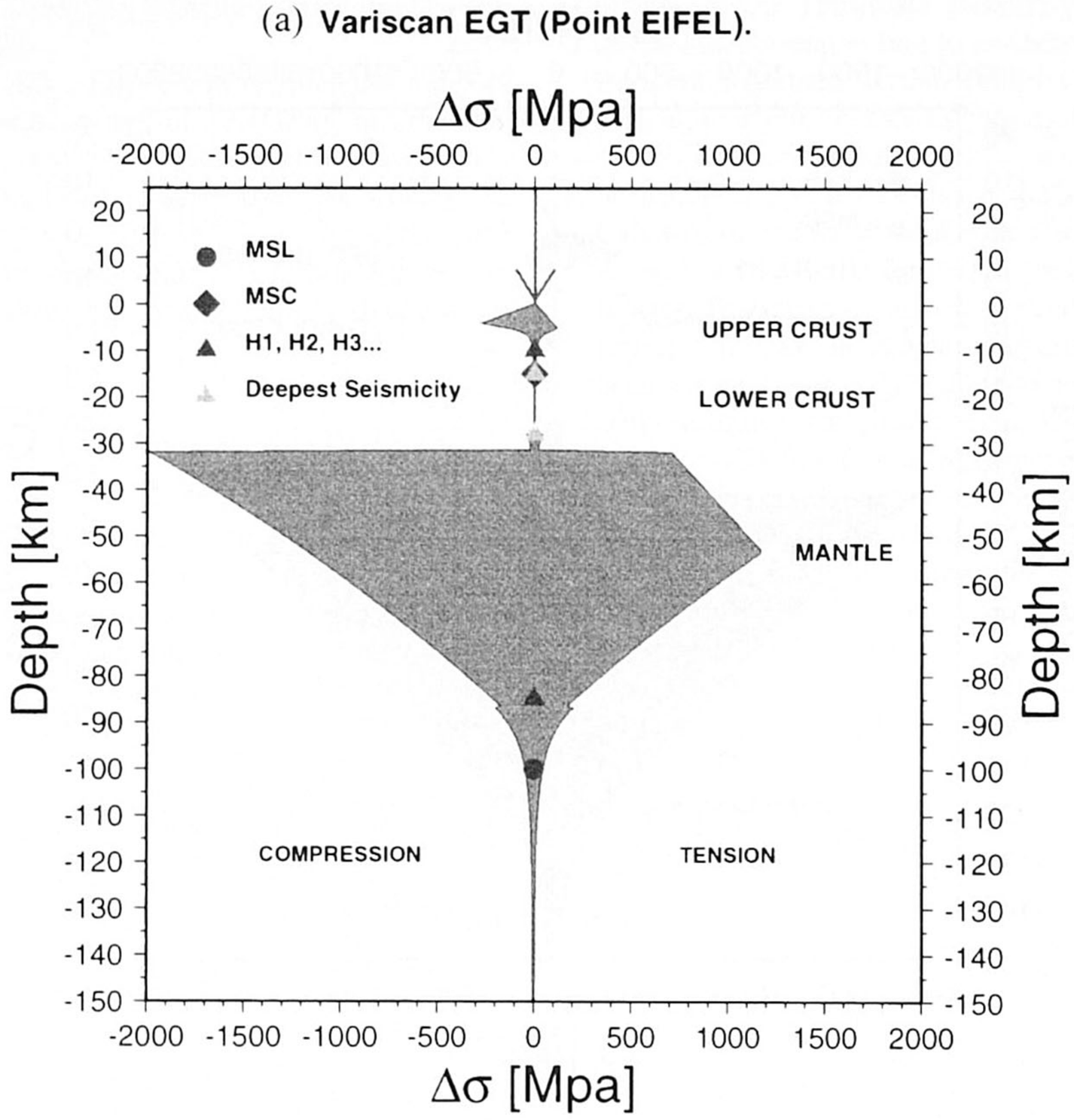

Figure 7. Predicted yield-strength envelopes for localities along the Variscan (central European) segment of the European Geotraverse (EGT). (a) Eifel; (b) North Hessian Depression; (c) Urach. Figure conventions as in Fig. 6.

crystalline complexes of the Moldanubian region of central Europe is still at an early stage (Franke 1992).

3.1.3 Alpine orogen: Aar, Molasse, Jura (Figs 1 and 8)

At the beginning of the Cretaceous period, the Adriatic microplate migrated eastwards with Gondwana, broke away and rotated anticlockwise. The resulting collision with Variscan European and the south-western margin of the East European Platform was followed by the initiation of the Alpine orogeny (Bertotti *et al.* 1993; Pfifner 1992). In the Jura mountain belt, seismicity is limited to the upper and lower crust (25–30 km), whereas seismicity in the Molasse basin reaches upper-mantle depths (Deichmann & Baer 1990). In the Aar–Gotthard regions, the seismic events are limited to a depth of 20 km (Deichmann & Baer, 1990; Cloetingh & Banda 1992). Using direct forward modelling, Royden (1993) and Kruse & Royden (1994) obtained EET values for the southern Alps (20 km), eastern Alps (40 km) and Apennines (10–15 km) (Fig. 10). On the basis of the data on the geometry of the basement, Bertotti *et al.* (1996) obtained somewhat lower but relatively consistent estimates for EET (from 5 km in the south to 25 km in the east). This discrepancy can be explained by the fact that Royden (1993) and Kruse & Royden (1994) used forward gravity modelling of plate flexure, principally limited both by the resolution of the Bouguer gravity data, which cannot resolve wavelengths smaller than the depth to the Moho, and by the assumption that the EET is constant along the model profile. Okaya, Cloetingh & Mueller (1996) inferred, from synthetic rheological profiles constructed on the basis of the local geophysical data, higher EET values for the southern Alps and slightly lower EET values for the northern Alps.

3.2 Eastern Europe and the FSU

3.2.1 Carpathians

The Carpathians present a 200-km wide fold and thrust belt convex to the east. This belt was formed in Miocene times, as a consequence of the underthrusting of the Russian platform beneath the European–Moesian platforms (Burchfiel & Royden 1982). The Pannonian Basin developed as a result of back-arc extension (Horváth 1993). Royden & Karner (1984) have used the depth to the crystalline basement of the Carpathian foreland basin to model the isostatic compensation for the presence of this mountain chain by a fractured elastic plate. They found that the EET is about 30 km, whereas the present load of the mountains appeared to be too low to explain the obtained magnitude of lithospheric deflections. They propose either the weight of the downgoing slab or dense mantle intrusions in the back-arc region as possible sources for the extra load. Vyskocil, Burda & Plancar (1983) revised the gravity data in the area and found that the Bouguer gravity anomalies should be corrected for low-density Tertiary sediments. As a result, additional loads applied to the plate are

(b) **Variscan EGT (Point NHD).**

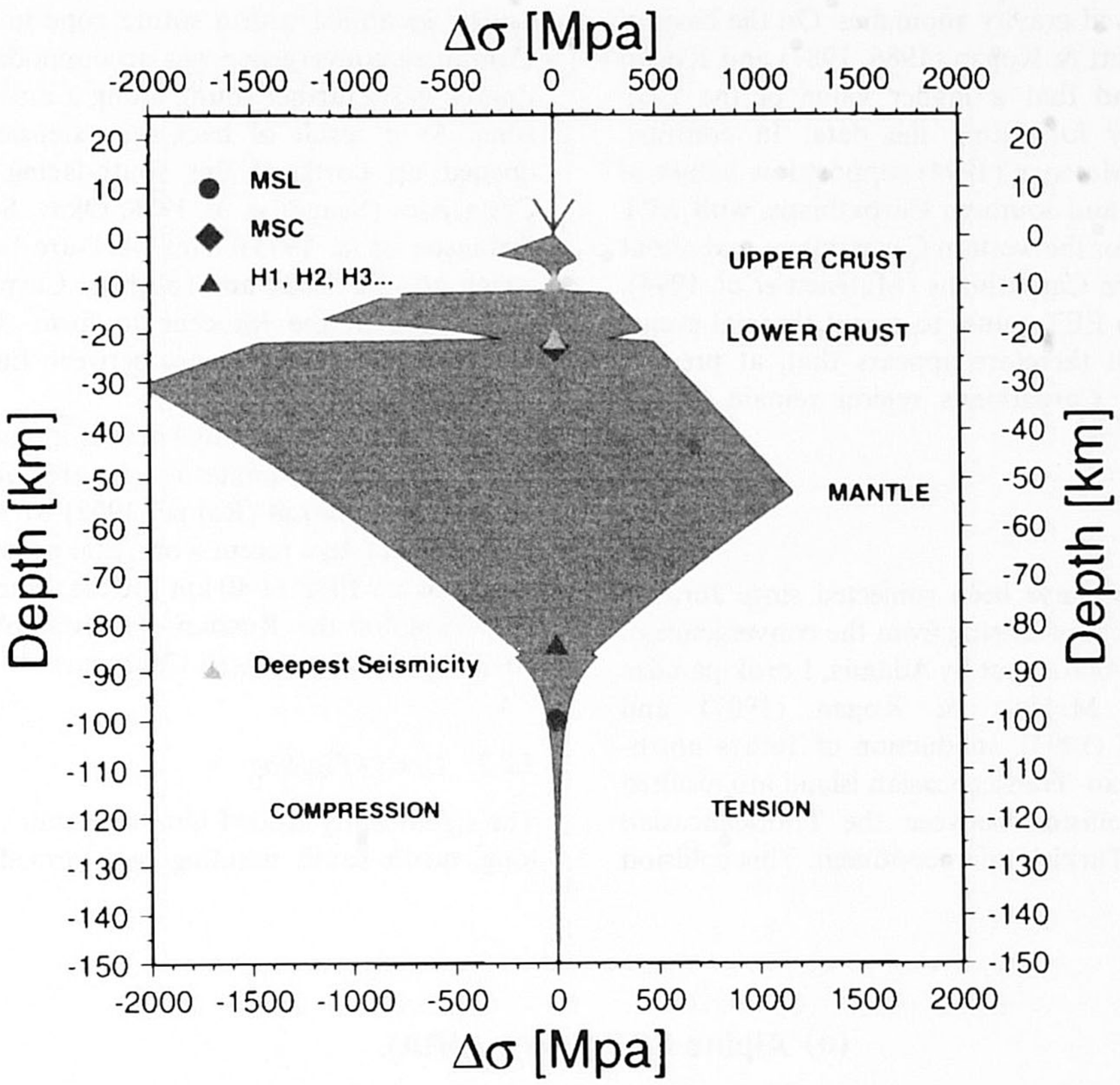

(c) **Variscan EGT (Point URA).**

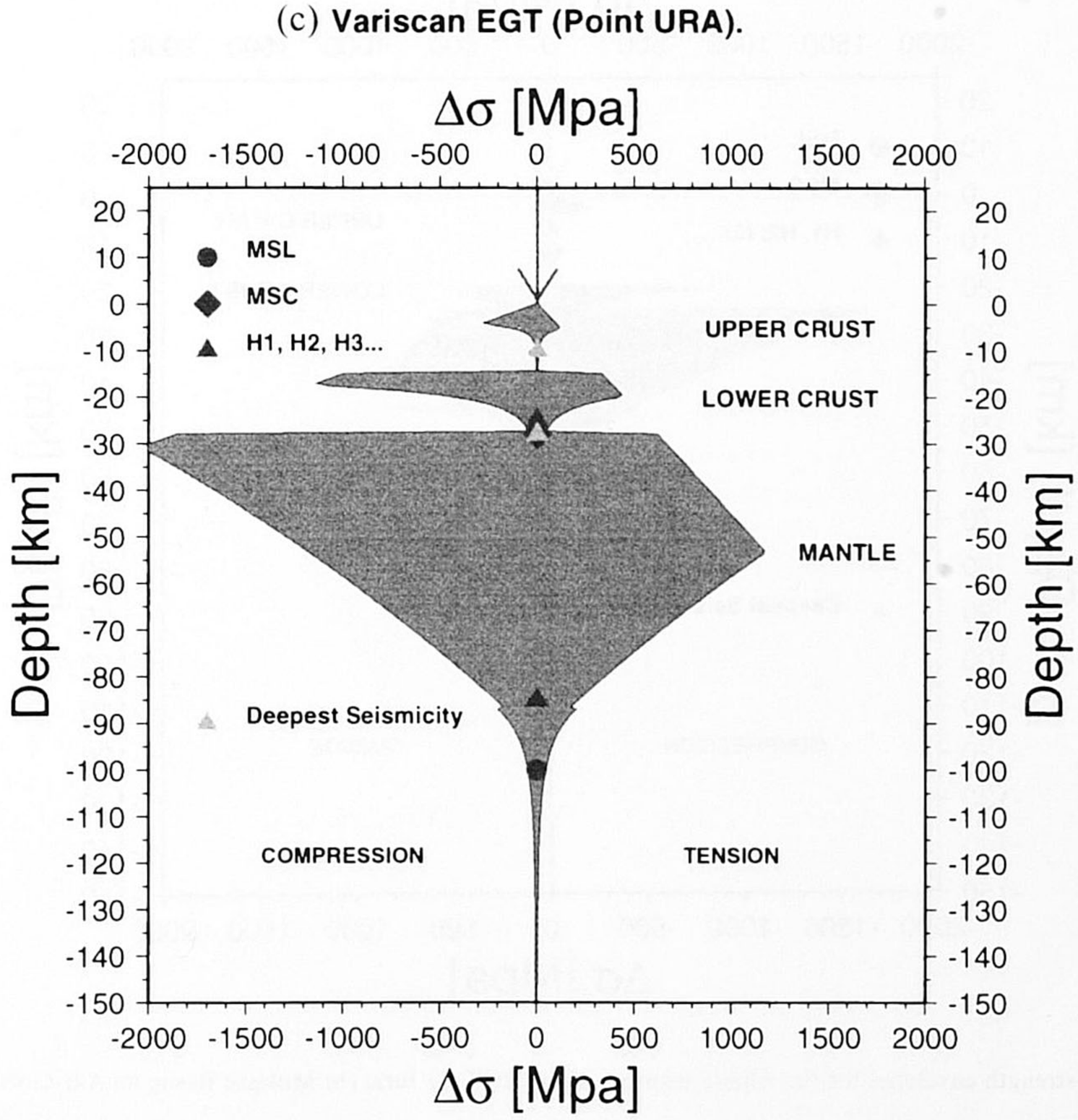

Figure 7. (*Continued.*)

required to fit the observed gravity anomalies. On the basis of these conclusions, McNutt & Kogan (1986, 1987) and Kogan & McNutt (1986) found that a higher value of the EET (EET = 40 km) is better for fitting the data. In contrast, Zoetemeijer, Tomek & Matencu (1994) support low values of the EET in the western and southern Carpathians, with EET values of about 5–8 km for the western Carpathians, and about 7–22 km for the southern Carpathians (Matencu *et al.* 1994). They attribute these low EET values to recent thermal events (including volcanism). It therefore appears that, at present, EET estimates for the Carpathians region remain poorly constrained.

3.2.2 *Caucasus*

The Caucasus mountains have been subjected since Jurassic times to intensive interactions arising from the convergence of Arabia and Eurasia. As pointed out by Adamia, Lordkipanidze & Zakaridze (1977), McNutt & Kogan (1987) and Stakhovskaya & Kogan (1993), subduction of Tethys northwards beneath the Pontian–Transcaucasian island arc resulted in a mid-Cretaceous collision between the Transcaucasian region and the Iranian–Turkish microcontinent. This collision can be identified with a suture zone in the Lesser Caucasus. Continued convergence was accommodated by closing of the Zagros basin further south, along a north-dipping subduction zone. As a result of back-arc extension, a marginal basin opened up north of this south-facing arc during the late Cretaceous (Sengör *et al.* 1988; Okay, Sengör & Görür 1994; Robinson *et al.* 1995). This back-arc basin, the remnants of which are the Black and southern Caspian seas, was uplifted and folded in the Miocene to form the Greater Caucasus during the final convergence between Eurasia and a salient in the Arabian plate.

The average crustal thickness is about 60 km (Belyayevsky 1974). The EET estimates for the area are quite controversial, ranging from 90 km (Ruppel 1992) to 36–83 km (McNutt & Kogan 1987). In a recent work, Stakhovskaya & Kogan (1993) proposed an EET of 40 km for the Arabian plate, an EET of 40–70 km for the Russian (Eurasia) plate, and an EET of 10–25 km for the western Caucasus.

3.2.3 *Urals (Fig. 9a)*

The significantly eroded Ural mountains constitute a 2000 km long, north–south trending belt formed during the collision

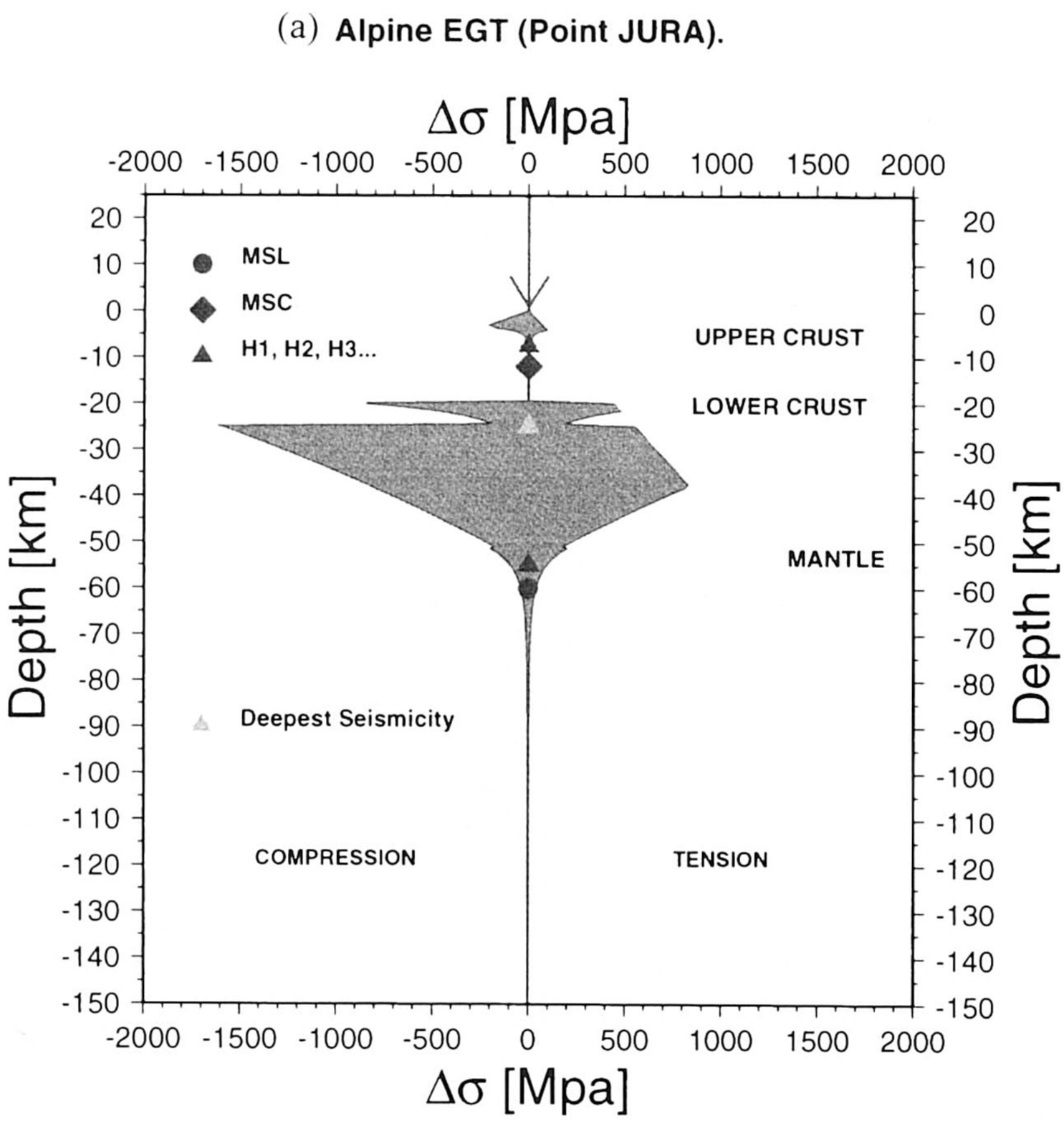

Figure 8. Predicted yield-strength envelopes for the Alpine segment of the EGT (a) Jura; (b) Molasse Basin; (c) Aar-Gotthard. Figure conventions as in Fig. 6.

(b) **Alpine EGT (Point MOLASSE).**

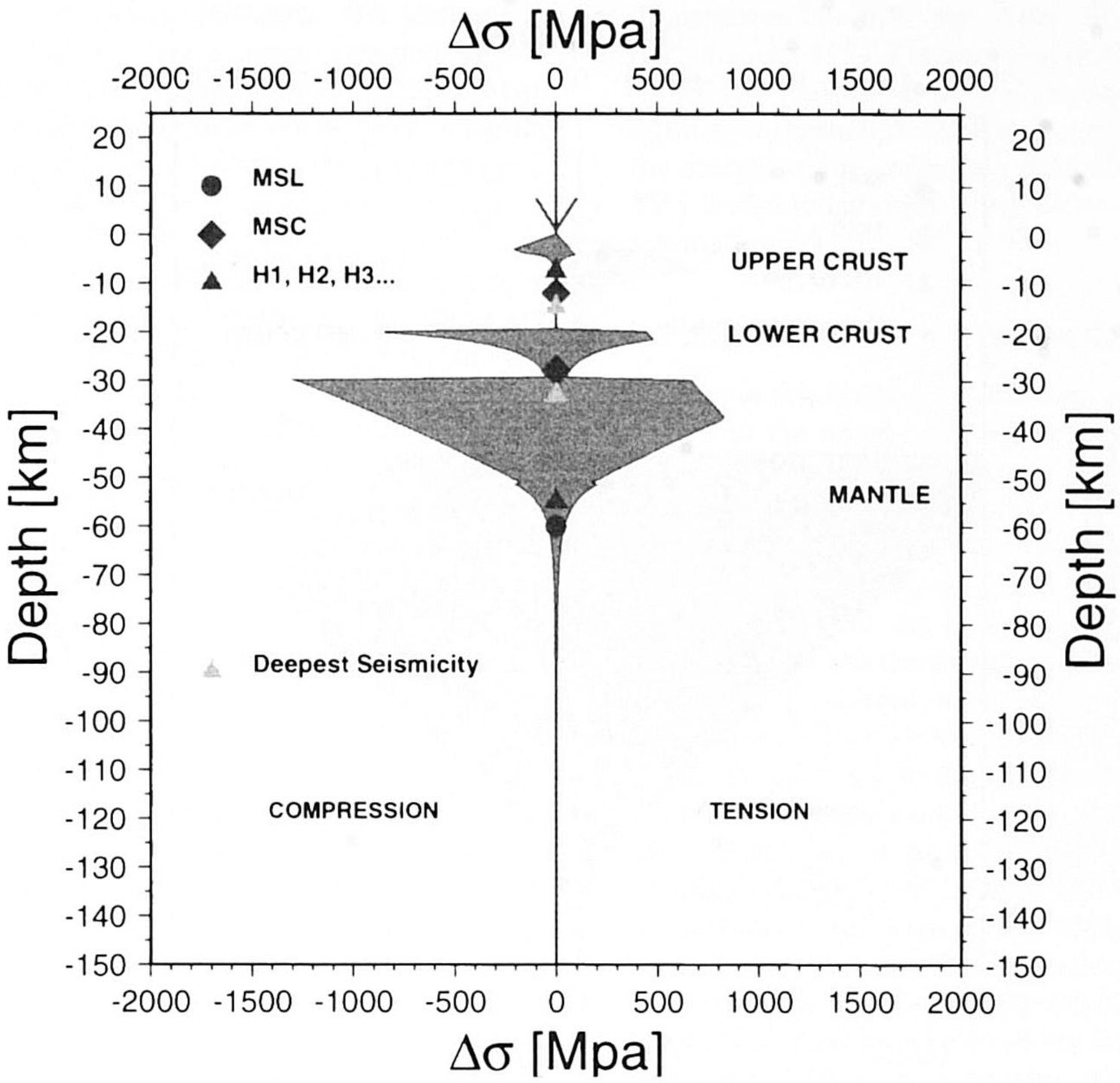

(c) **Alpine EGT (Point AAR).**

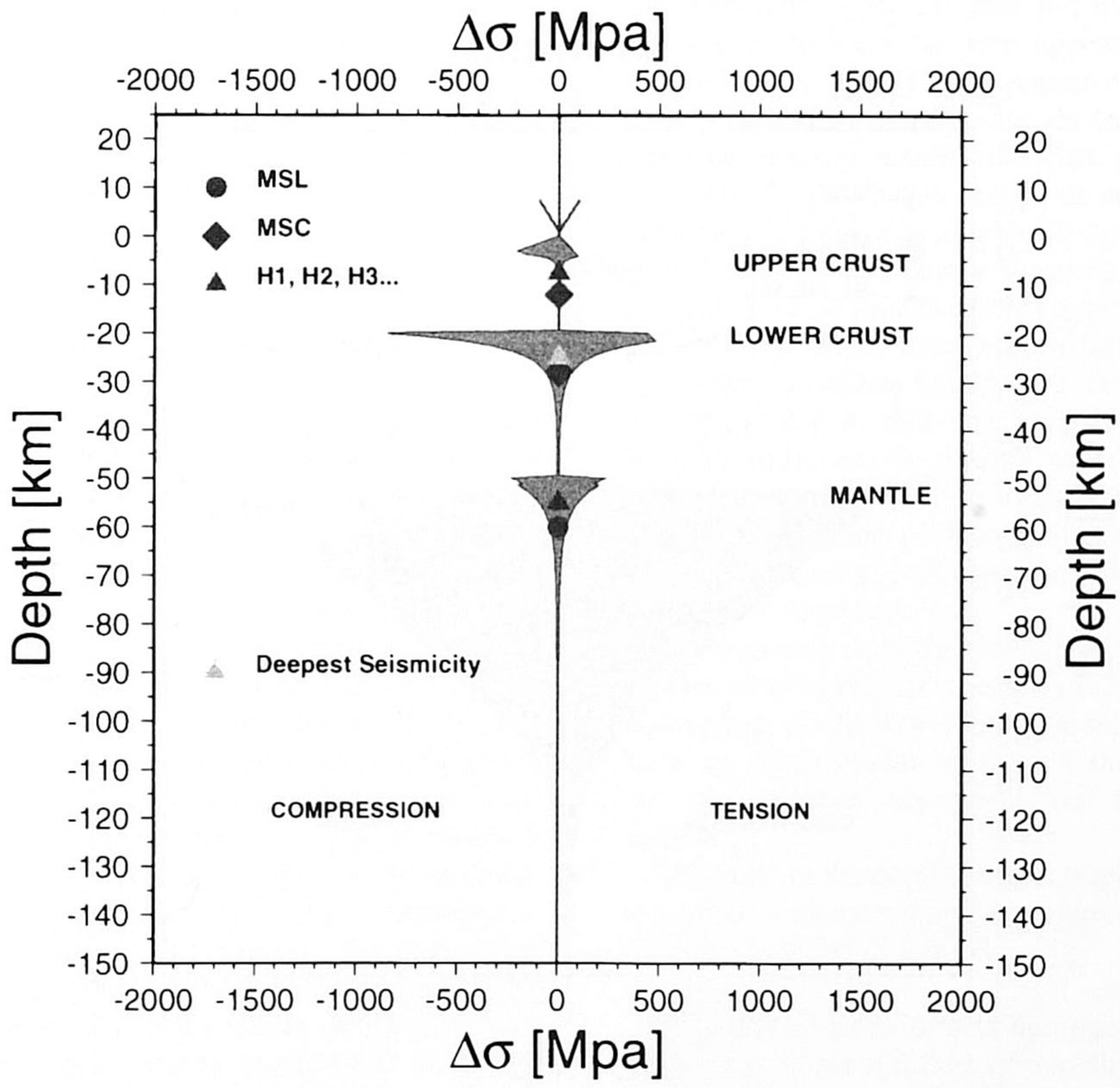

Figure 8. (*Continued.*)

(a) **URALS.**

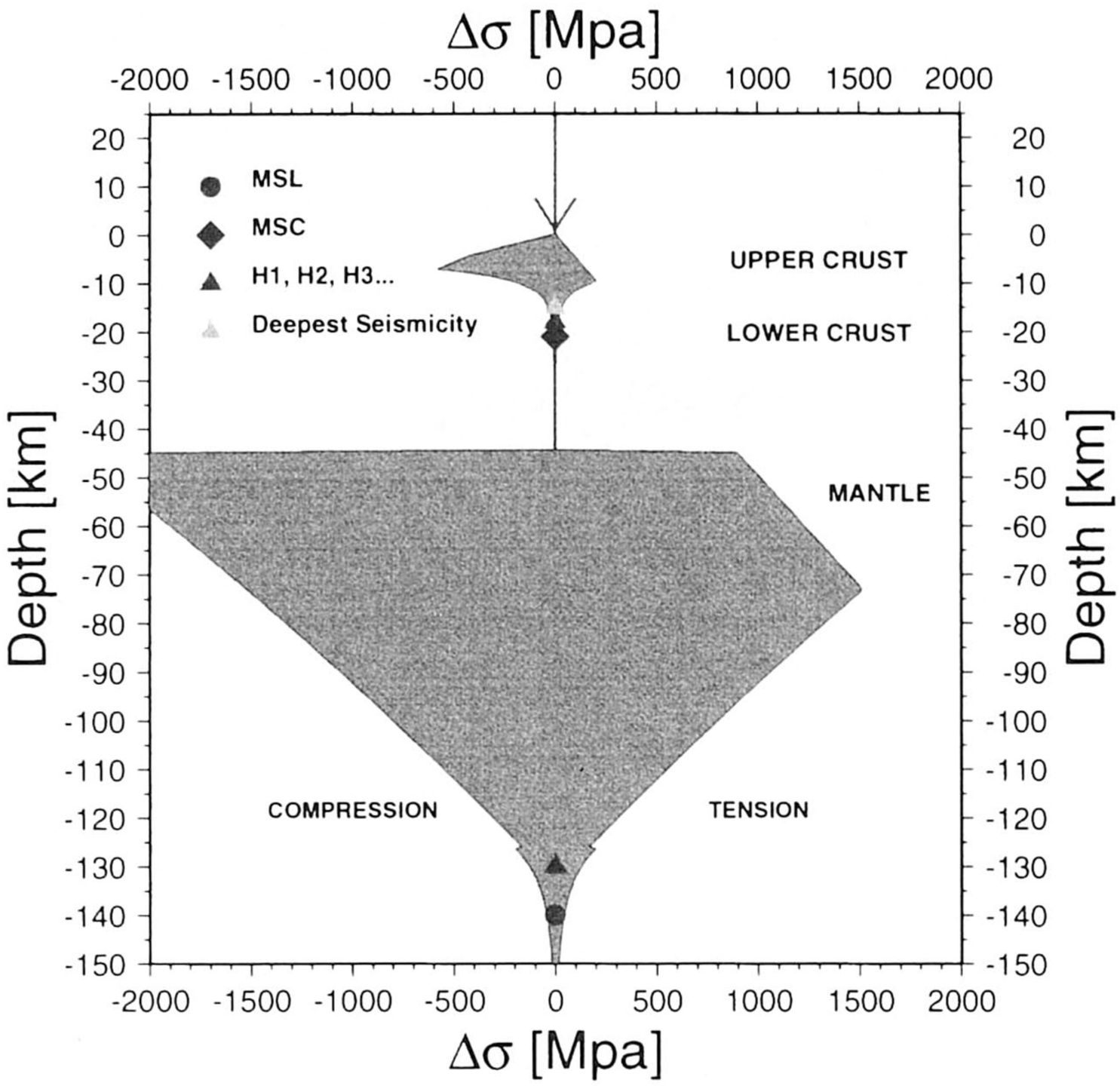

(b) **TARIM.**

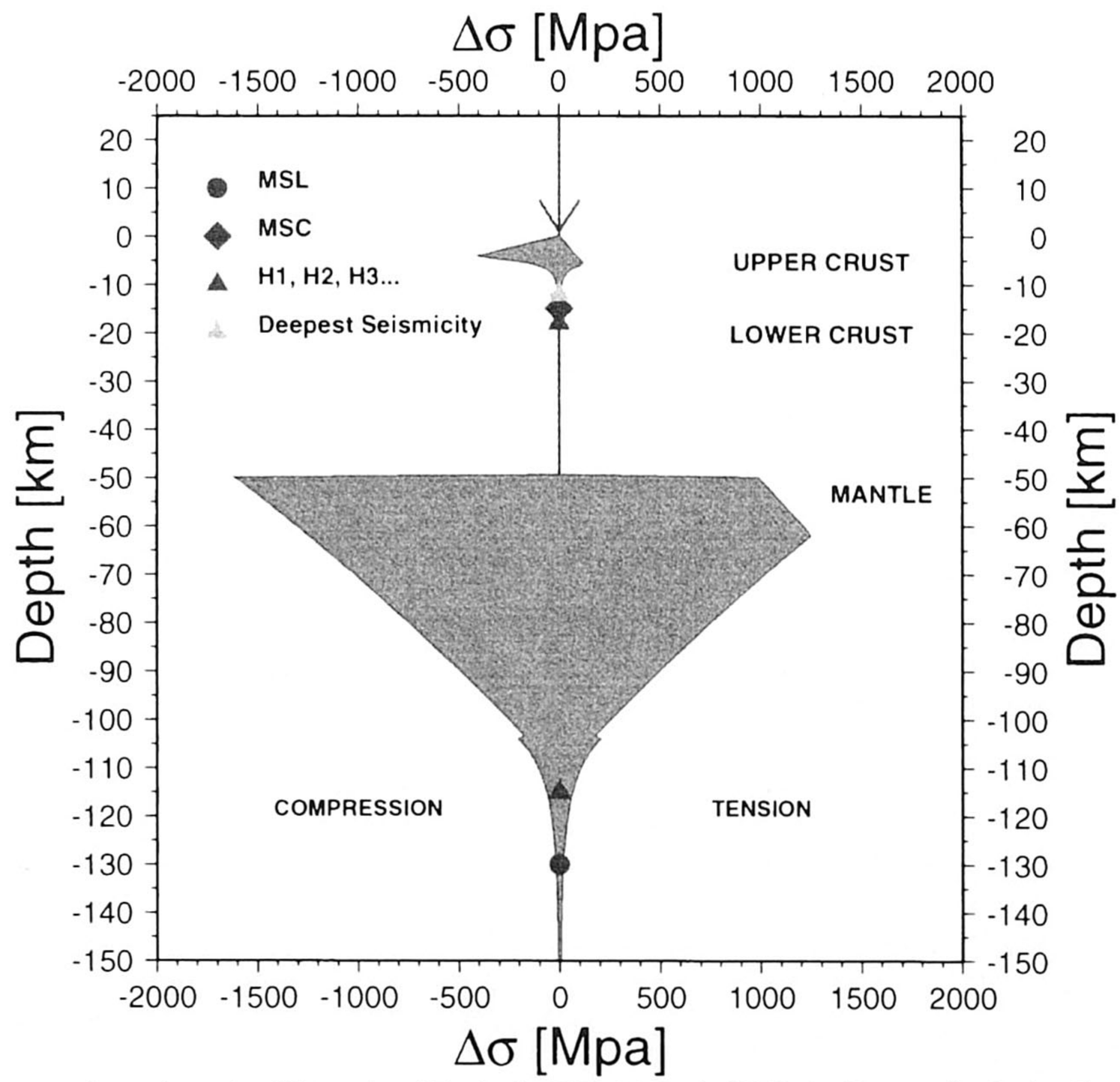

Figure 9. Predicted yield-strength envelopes for different localities in the FSU. (a) Urals; (b) Tarim/Dzungarian basin. Figure conventions as in Fig. 6.

between the Russian and Siberian platforms. The foreland to the west dips over the East European craton. The thickness of terrigenous sediments filling the foredeep basins exceeds 5 km. The eastern foreland extends out over the western Siberian lowlands. It contains tight, flattened folds, mostly eroded and buried (Sokolov 1992). The absence of andesites in the western Ural foreland and polarity of paired middle Paleozoic metamorphic belts confirm an eastward dip for the subduction zone between the converging Russian platform and an island arc off the Siberian coast during the Ordovician and Silurian. The eastward-dipping Main Ural Deep Fault was active around 400 Ma ago. At present, it marks the major suture between continental rocks of the East European platform and the oceanic melange which finally collided in Early Devonian–Permian times (Plyusnin 1963). The two continents finally collided in the Permian. According to the age maps for the western Siberian lowlands adjacent to the Urals (Sclater *et al.* 1981) and K–Ar dates from deep boreholes (Hamilton 1970), the age of the basement at the time of loading is early Palaeozoic. The deep seismic sounding data and gravity data detect the presence of thick crust of 40 to 50 km (e.g. Kunin, Sheih-Zade & Semenova 1992). The heat flux data show good consistency (Smirnov 1980) with the plate-cooling model.

Various authors (e.g. McNutt & Kogan 1987; Kruse & McNutt 1988; Stakhovskaya & Kogan 1993) have proposed that, during the final phase of the continent–continent collision, the east European platform underthrust the mountains from the west, perhaps by reactivating the Main Ural Deep Fault. According to this explanation, the gravity high peaking about 800 km to the west of the Urals, and continuous along strike of the mountains farther north (Bowin, Warsi & Milligan 1981; Kruse & McNutt 1988), reflects a flexural arch from loading. The approximate elastic thickness of the plate, obtained from direct elastic-plate modelling, constrained by a newly available high-resolution ($5' \times 5'$) gravity data set, is 75–90 km (Stakhovskaya & Kogan 1993). The extra load of the dense ophiolites could obviously maintain the Ural foredeep and arch for hundreds of millions of years, in spite of the deep erosion of the Ural topography.

3.2.4 Tarim-Dzungaria (Fig. 9b)

The Precambrian to Palaeozoic Tarim and Dzungaria basins bound the Tien Shan range to the north and south-east, respectively. Although the strata in the Tien Shan were intensively deformed in Late Palaeozoic times (e.g. Burtman 1975; Babaev *et al.* 1978; Burov *et al.* 1990), when the Tarim block of Precambrian rock apparently collided with Siberia, relief associated with that belt was eroded in Cenozoic times (e.g. Hendrix, Trevor & Graham 1994). The rate of convergence of the Tarim block and Siberian/Kazakh shield is between 5 and 20 mm y^{-1}. This corresponds to an average strain rate of about 3×10^{-15} s^{-1}. The relatively deep Dzungarian basin north of the Tien Shan in China appears to be structurally similar to the basins along the southern margin of the chain. It has been proposed that the basement of the Dzungarian basin is underthrusted northwards beneath the Tien Shan (e.g. Benedetti 1993). The EETs of the lithosphere underlying these basins are quite similar, with values of about 65 km (Lyon-Caen & Molnar 1983; Burov *et al.* 1990; Burov & Diament 1992; Benedetti 1993). The crustal thickness of the lithosphere beneath the Tien Shan is about 50–70 km (Belyayevsky 1974; Babaev *et al.* 1978; Volvovsky & Volvovsky 1975). The heat flux data (Smirnov 1980) demonstrate no significant thermal anomalies except probably to the north of the central and western Tien Shan (Kazakh shield), where the EET is also remarkably lower ($\sim$10–15 km), suggesting recent thermal events.

4 RHEOLOGY AND SEISMICITY

Intraplate seismicity in continental areas is frequently associated with the upper crust, while it is frequently assumed that the lower crust is too weak to have any remarkable brittle strength (e.g. Chen & Molnar 1983). The most commonly inferred mechanism of seismicity is the development of frictional instabilities on sliding surfaces (faults, cracks). Consequently, it is assumed that the material should be brittle or brittle–elastic to allow the development of such instabilities. A number of recent studies have indicated the presence of seismic events in the lower crust as well as in the upper mantle, although practically everywhere the number of events in the lower crust is much lower than observed in the upper crust (Shudofsky 1985; Shudofsky *et al.* 1987; Deverchere *et al.* 1991, 1993; Cloetingh & Banda 1992; Doser and Yarwood 1994). Although seismogenic lower crust is now well detected in a number of regions, there are very few indications of seismicity and faults just below it, at upper-mantle levels (Cloetingh & Banda 1992). One of the possible explanations for this is that the mantle may be weaker than is usually supposed due to the lower activation energy values mentioned in Section 2. However, the assumption of weak mantle rheology does not hold in the areas with high and average values of the effective elastic thickness (EET $\sim$ 40–110 km). For these areas, the most obvious explanation for the rare appearance of the low crustal seismicity is a possible crust–mantle decoupling by weak lower crust (Figs 3 and 4). In this case, the transition of the differential stress between the mantle and crust is interrupted by a ductile low-viscosity channel in the lower crust. Fig. 4(b) shows, for example, that, at considerable flexural deformation, bending stresses may exceed ductile limits in the lower crust, thereby inducing flow by ductile creep. On the other hand, the flexural stress in the upper mantle is probably not high enough to exceed brittle failure limits there. It is shown in Section 5.1 and Appendix A that the vertical gradient of differential bending stress can be directly calculated from the observed radius of plate flexure, and vice versa. Therefore, from the direct observations of flexure it seems possible to predict potentially optimal conditions for upper crustal, lower crustal and mantle seismicity.

The presence of horizontal far-field stresses in Europe (see Müller *et al.* 1992 for a discussion) may also result in the decoupling of the crustal and mantle lithosphere and thus have an effect similar to that of the bending stress (Fig. 4, see also further discussion on the effects of far-field stresses).

The cases of the deep crustal intraplate seismicity are mostly associated with extensional tectonic regimes. The cases can be roughly classified as follows:

(1) zones of more or less homogeneous lower-crustal seismicity (e.g. Albert rift, East Africa: Shudofsky 1985; Shudofsky *et al.* 1987; Morely 1989; Seno & Seito 1994);

(2) zones of localized deep seismicity, generally with localizations along deep faults (Baikal rift: Deverchere *et al.* 1991; Rhine graben: Fuchs *et al.* 1987; Brun *et al.* 1991, 1992).

This differentiation can be related to various conditions associated with seismogenic stress release. There are several possible explanations for the occurrence of seismicity in the lower crust.

(1) More 'basic' composition (Stephenson & Cloetingh 1991; Cloetingh & Banda 1992). In areas where the lower crust consists of minerals with a low temperature of creep activation (diabase, diorite etc.), it may remain brittle at depths corresponding to the depth to 300–400 °C (20–35 km); the other possible reason lies in compositional differences in the lower-crustal material (e.g. Sibson 1980, 1982).

(2) Variation of unstable-to-stable frictional slip on the deeply penetrating faults (Tse & Rice 1986). It is important to note that the brittle–ductile transition refers to a bulk rheological property, while the earthquakes are associated with frictional instabilities. Localized strain-rate acceleration along the faults can keep quartz-controlled material brittle, even at Moho depths (40–50 km), according to some recent numerical tests (A. Poliakov & Y. Podladchikov 1993, personal communication). Such deep faults penetrating to the mantle lithosphere are observed, for example in the Northern Baikal rift (Deverchere *et al.* 1993).

(3) Non-brittle mechanisms of seismogenic stress release. This may be related, for example, to unstable phase changes, re-orientation of the crystalline grid of minerals and to a few other mechanisms that are the subject of intensive discussions (Kirby, Durham & Stern 1991; see also Govers *et al.* 1992 for a review).

Unfortunately, seismic patterns do not allow discrimination between the brittle and hypothetical non-brittle (ductile) earthquakes. The almost complete absence of earthquakes beneath the seismic Moho remains difficult to explain. Our possible explanations include stress relaxation due to crust/mantle decoupling; strengthening of the uppermost mantle due to downward bending (in downward-bent rift basins); or low or inhomogeneous horizontal intraplate stress. As shown in Fig. 4, due to the typically thick continental crust and crust–mantle detachment, the bending stresses at the crust–mantle boundary are much lower than the yield strength, as the weight of the thick crust significantly increases the brittle strength of the mantle lithosphere. Therefore, in the continents the brittle yield limits of the mantle lithosphere cannot be reached as easily in the oceans. Alternatively, the mantle lithosphere may not be so ductilely strong as previously suggested. The lithospheric strength is usually measured in terms of the EET, and it appears that the EET in the young active collision zones follows the depths to an isotherm of 200–300 °C marking the base of the mechanical crust (Fig. 10). This suggests that the mantle portion of the lithosphere is almost ductile there. Another possible explanation, according to Kirby *et al.* (1991), may be the inapplicability of Byerlee's law of brittle failure at depths in excess of 50 km. Therefore, in regions with thick continental crust (40–60 km), the uppermost mantle could be too deep to obey Byerlee's law. For the upper crust, deep drilling has recently provided direct evidence in support of Byerlee's law (Zoback *et al.* 1993).

5 EET ESTIMATION: DIRECT ESTIMATES AND THEORETICAL PREDICTIONS

5.1 EET (T_e) as a function of the thermotectonic age (temperature), strain rate, composition, flexure, and horizontal force

The implication of the effective elastic thickness EET (T_e) of the lithosphere is based on the known hypothesis that the gravitational equilibrium of the lithosphere over geological time and space scales is analogous to the flexure of a thin competent (elastic) plate overlying an inviscid fluid asthenosphere. Most of the generally used analytical and numerical models of the mechanical behaviour of the lithosphere consider it as a closed system with a 'black box' response to external parameters: vertical loads, or density variations (i.e. mountain belts, magmatic underplating), forces (due to horizontal far-field stresses), and bending moments (related to plate curvature) are used as input, and substratum (crystalline basement) geometry or deflections of the Moho and gravity anomalies are the output (e.g. Watts & Talwani 1974; Forsyth 1980; McNutt 1980; Lyon-Caen & Molnar 1983; De Rito, Cozzarelli & Hodge 1986; Sheffels & McNutt 1986; Watts & Torne 1992). Irrespective of the real strain and stress distributions occurring within the deformed lithosphere, one can always estimate an 'effective' elastic (plastic, or visco-elastic) plate thickness that will relate the output to the input. Such best-fitting apparent EET values will be referred to as '*observed*' or '*direct*' EET estimates of the lithosphere.

On the other hand, one can also *theoretically* predict EET on the basis of the data on the rheology of the lithosphere (Section 2), heat flow, plate kinematics, seismic data, MT and gravity data, and observations of plate flexure. Comparison of the observed EET with the theoretical predictions can provide independent information on the plate structure, its thermal history, as well as constraining experimentally derived rheological laws themselves.

To predict regional and local EET values from rheological profiles, we use the method for estimation of the EET of a non-elastic plate that was originally proposed by Burov & Diament (1992, 1995) and is briefly summarized in Appendix A. According to this approach, the EET can be directly expressed through the integral of the yield-stress envelope $\sigma(\varepsilon)$ with depth, local plate curvature and horizontal force acting on the plate. In this formulation, the mechanical thickness of the plate is the upper limit of integration. When the EET is known, it is then possible to recalculate the mechanical thickness of the lithosphere. As shown in Fig. 5, the knowledge of the mechanical thickness is of fundamental importance because it allows us to bound the uncertainties in prediction of the rheological structure of the lithosphere to maximal 20 per cent.

Fig. 10 shows the compilation of the European and Eurasian EET estimates obtained from direct modelling and from rheological predictions constrained by seismically/rheologically predicted MSC, MSL and h_1, h_2, h_3 estimates. These data are also compared with a conventional thermal model of the continental lithosphere. As demonstrated in Fig. 10, in the absence of a clear correlation of EET with any specific isotherm, the quantities MSC, MSL, and h_1, h_2, h_3 demonstrate a strikingly good correlation with the position of the 200–300 °C and 700–800 °C isotherms, respectively. A good correlation can also be observed with the depth of the deep intraplate seismicity.

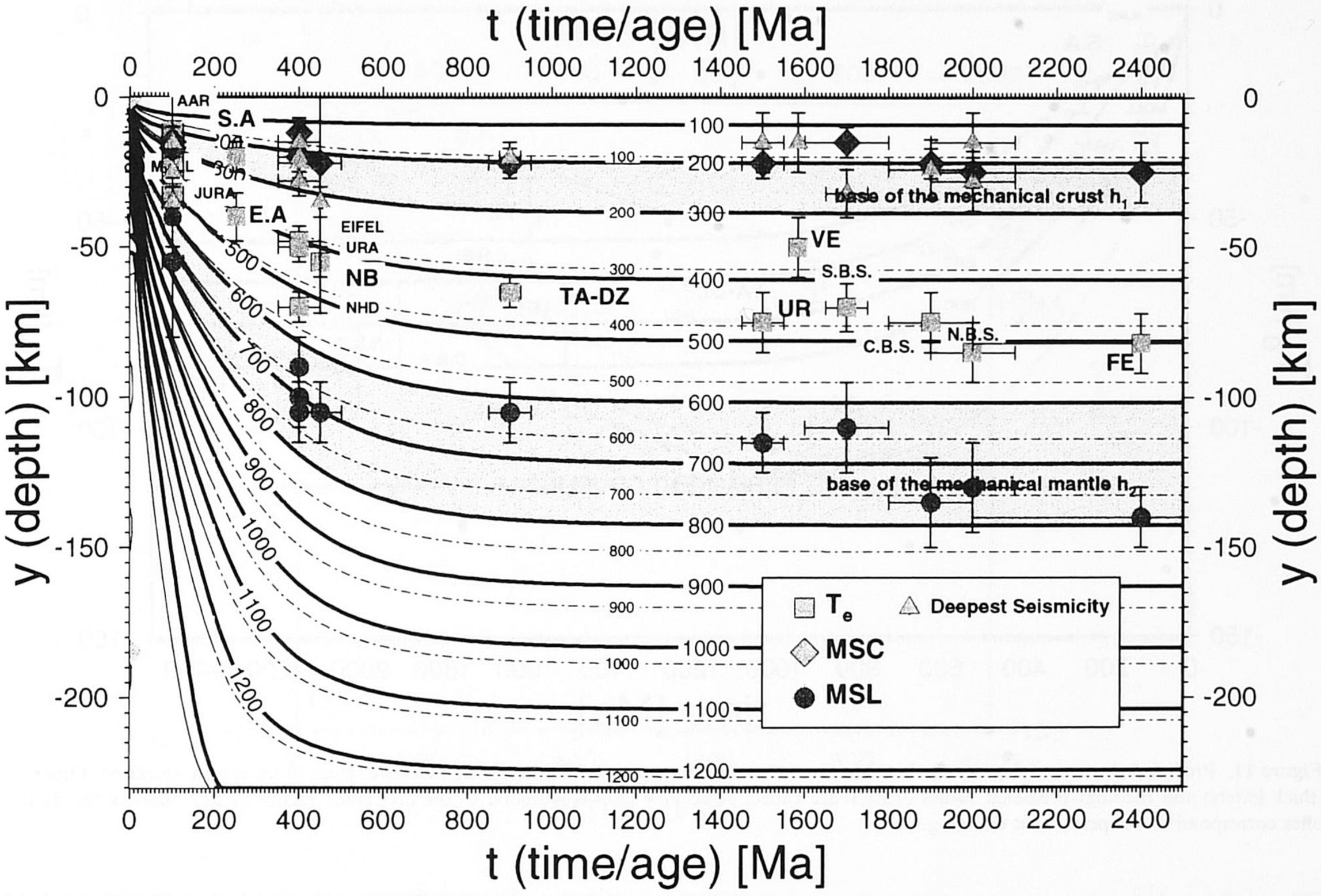

Figure 10. Compilation of the observed and predicted values of EET, MSC (depth to the bottom of mechanically strong crust) and MSL (depth to the bottom of mechanically strong mantle lithosphere) against the age of the continental lithosphere at the time of loading and the thermal model of the continental lithosphere. The squares correspond to EET estimates; circles to MSL estimates; and diamonds to estimates of MSC. Thick solid letters correspond to directly estimated EET values obtained from flexural models ('observed' EET); thinner solid letters are used for indirect rheologically derived EET estimates. Notations for sites are as in Fig. 1. Isotherms marked by solid lines are for the model that accounts for the additional radiogenic heat production in the upper crust. The dashed lines correspond to pure cooling models for continental lithosphere. The equilibrium thermal thickness of the lithosphere is 250 km. The shaded bands correspond to the depth intervals marking the mechanical base of the crust (MSC) and the mantle portion (MSL) of the lithosphere

The data set includes:

Old thermomechanical ages of 1000–2500 Ma

Northernmost, Central, and Southernmost Baltic Shield (predicted EET); Fennoscandia (direct EET estimates) (Cloetingh & Banda 1992; Morner 1990); Verkhoyansk plate (McNutt *et al.* 1988); Urals (Stakhovskaya & Kogan 1993); Carpathians (Royden 1993; Zoetemeijer *et al.* 1994; Matencu *et al.* 1994); Caucasus (Stakhovskaya & Kogan 1993).

Intermediate thermomechanical ages of 500–1000 Ma

North Baikal (Burov & Diament 1995); Tarim (Lyon-Caen & Molnar 1984; Burov *et al.* 1990); Dzungaria (Benedetti 1993) (direct EET estimates); Variscan of Europe: URA, NHD, EIFEL (rheologically predicted EET) (Cloetingh & Banda 1992).

Younger thermomechanical ages of 0–500 Ma

Alpine belt, Jura, Molasse, Aar (predicted EET) (Cloetingh & Banda 1992); southern and eastern Alps (direct EET estimates) (Royden 1993); Ebro Basin (Zoetemeijer *et al.* 1990); Betic rift margin (Peper & Cloetingh 1992); Betic Cordilleras (van der Beek & Cloetingh 1992; Cloetingh *et al.* 1992).

5.2 EET and thickness of the crust and mantle lithosphere

The crust–mantle decoupling can result in a drastic reduction (up to two times) of the total effective strength of the lithosphere (McNutt *et al.* 1988; Burov & Diament 1992). This effect may be demonstrated by a simple analogue with a multilayer elastic plate. The effective elastic thickness of a plate, consisting of n detached (non-welded) competent layers is (Burov & Diament 1995)

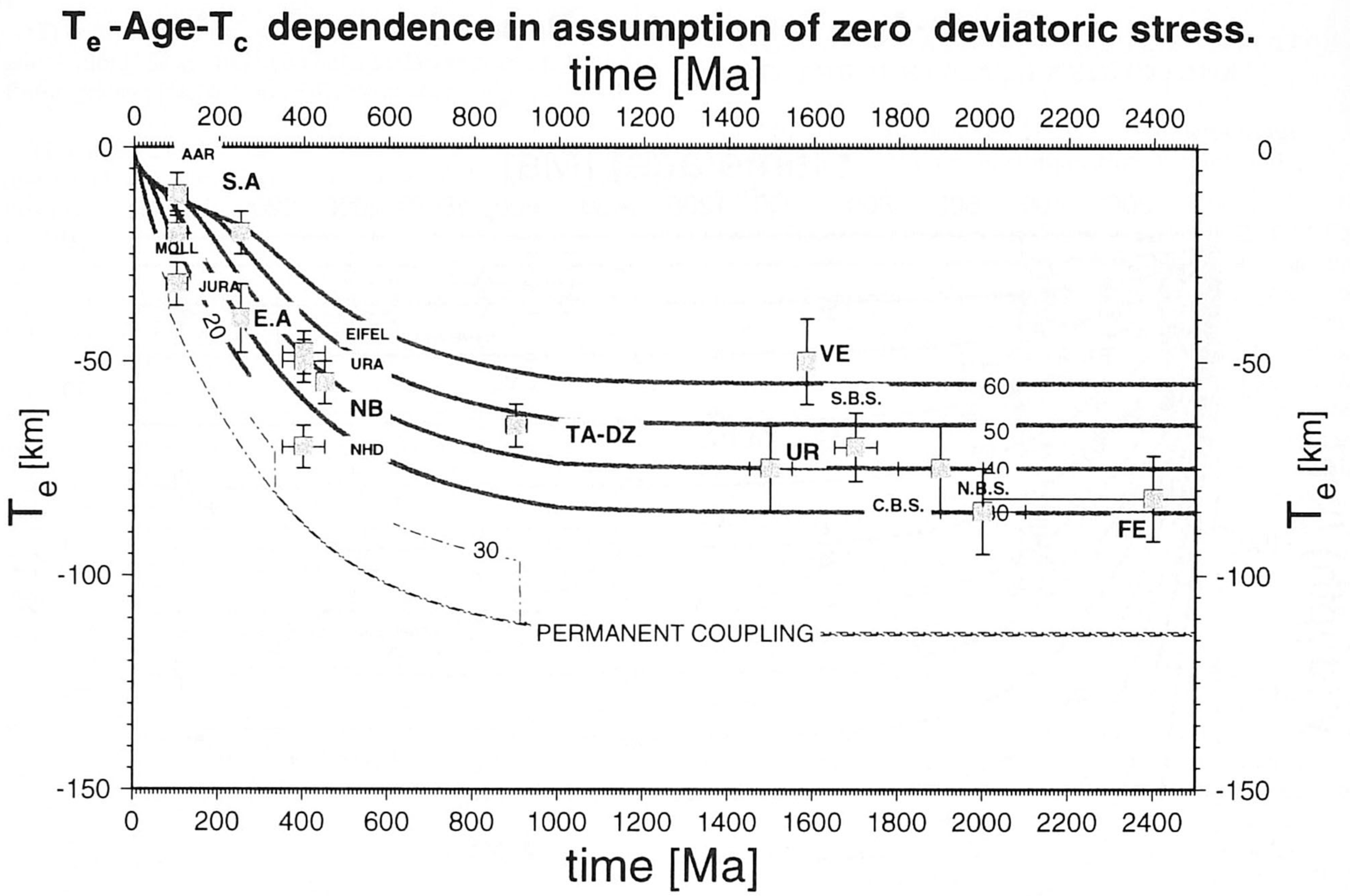

Figure 11. Predicted theoretical dependence between the thermotectonic age and EET assuming different values of the crustal thickness. Observed (thick letters) and rheology-predicted values of EET are added. Solid grey lines correspond to the decoupled regime of deformation; the dashed ones correspond to the permanent coupling.

$$T_e^{(n)} = \left(\sum_{i=1}^{n} \Delta h_i^3 \right)^{1/3},$$

where $\Delta h_i = y_i^+ - y_i^-$ is the effective elastic thickness of the ith layer. For example, the total elastic thickness (T_e) of decoupled two-layer lithosphere with the base of the competent upper crust at depth $y_1^- = h_1$, the base of the competent mantle at depth $y_2^- = h_2$, and with a total thickness of the crust $y_2^+ = h_c$, $h_c > h_1$ (e.g. McNutt *et al.* 1988, see Appendix A for notation) is

$$T_e^{(2)} = \sqrt[3]{h_1^3 + (h_2 - h_c)^3} \approx \max(h_1, (h_2 - h_c)). \qquad (5.1)$$

If the thickness of the competent crust (h_1) is equal to the thickness of the competent upper-mantle layer ($h_1 = h_2 - h_c$), then $T_e^{(2)} = 1.26(h_2 - h_c)$; if it is only half of the thickness of the competent mantle $[h_1 = 0.5(h_2 - h_c)]$ then $T_e^{(2)} = 1.04(h_2 - h_c) \approx (h_2 - h_c)$. For the coupled rheology, where crustal and mantle layers are 'welded' together, the EET of the plate will be simply equal to h_2.

It is important to note that h_1 and h_2 are defined as the depths at which the yielding strength does not exceed 1–5 per cent of the lithostatic pressure. Therefore h_1, h_2 do not exactly coincide with the depths to the critical geotherms 300 °C and 750 °C, but depend as well on the slope of the yield-stress envelope in the vicinity of depths corresponding to these temperatures. Figs 11 and 12 show predicted EET values for non-loaded lithosphere, compared with available direct EET estimates. These estimates are obtained from the synthetic rheological profiles shown in Figs 6, 7 and 8. For example, the estimates for the EET, made on the basis of these data are 48 km for the Eifel, 70 km for North Hessian Depression and 50 km for Urach. A systematic correlation can be observed between the theoretically predicted values for EET and the values inferred from observations of flexure.

5.3 Effect of a moderate in-plane and normal stress

The absolute values of the horizontal intraplate stress are not known. However, according to most estimates, a compressive horizontal stress level of 75–200 MPa is sufficient to activate whole-lithosphere folding of the young crust-controlled lithosphere as observed in the Eurekan belt of Arctic Canada (e.g. Stephenson & Cloetingh 1991). Stress levels of about 500 MPa would be required for an older lithosphere. Therefore, for the areas where prominent folding is not observed, it is likely that the level of the vertically averaged compressive horizontal stress does not exceed 100–500 MPa, although it is possible that localized stress fluctuations (superimposed bending stress) at some depths may exceed the average value in a few places (Kusznir 1991) (Fig. 4). Fig. 13 shows the effect of overall horizontal stresses on the value of EET. One can see that stress variation by 100–200 MPa leads to a variation of the EET comparable with a shift of the critical isotherms by approximately 50–100 °C (~5–10 per cent change in EET for

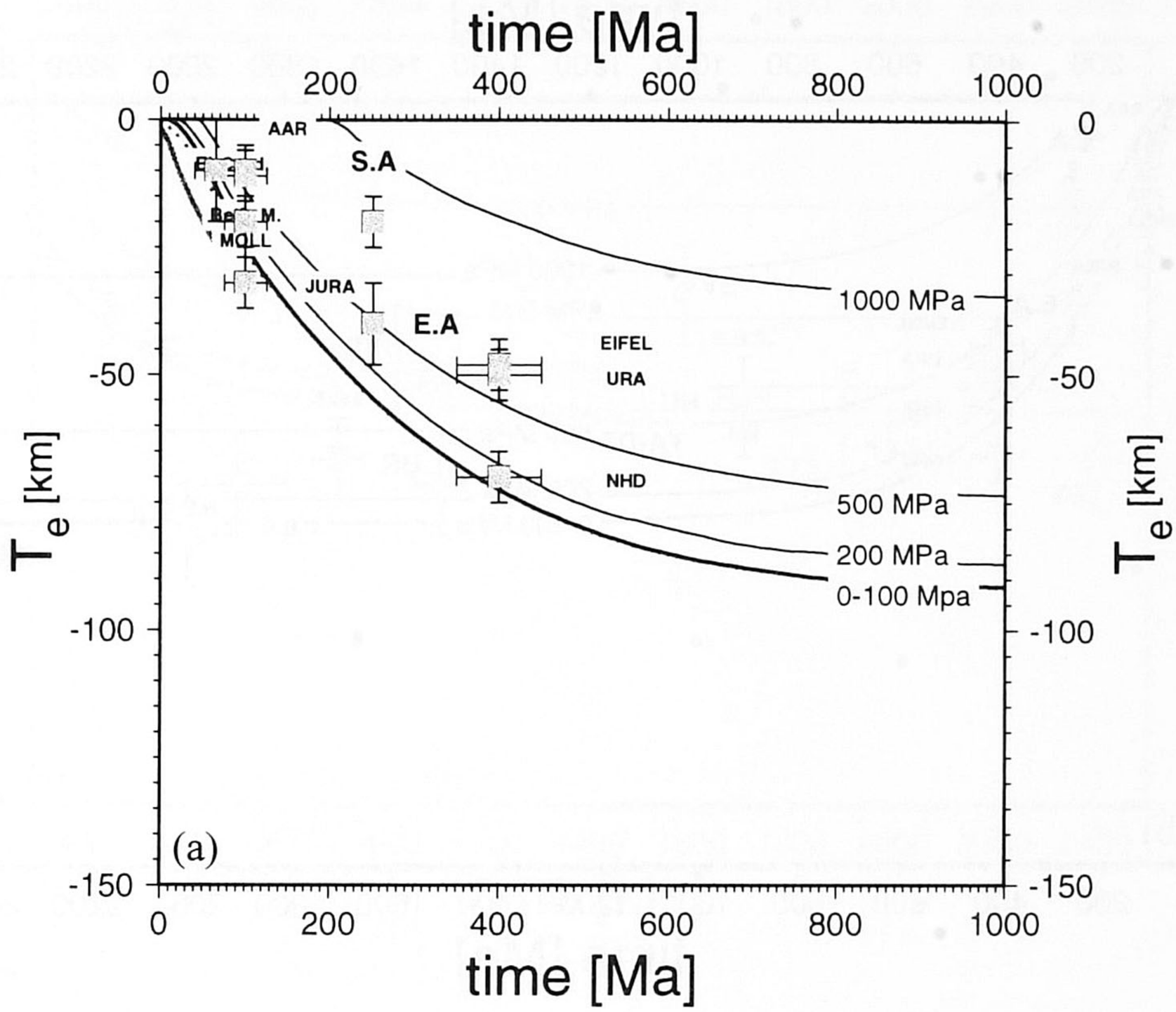

Figure 12. As Fig. 11, but with the effect of intraplate stresses shown, and EET (T_e) estimates clustered by groups with close crustal thickness (T_c) values (30, 40, 50 km). (a) Crustal thickness of about 30 km; (b) crustal thickness of 40 km; (c) crustal thickness of 50 km.

old stable lithosphere, and larger changes for young lithosphere). Indeed, the averaged value $\bar{\gamma}$ of the slope γ of the ductile mantle part of the yield-strength envelope [$\gamma = \sigma(\varepsilon)/dy$], shown in Fig. 6(a), is approximately 20 MPa km^{-1}. A horizontal stress $\Delta\sigma$ of 200 MPa will shift the mechanical bottom of the mantle lithosphere by a value $\approx \Delta\sigma/\bar{\gamma}$, that is 10 km, or about 10–15 per cent of the initial mechanical thickness of the mantle lithosphere. A comparison with Fig. 10 shows that, for the age range of 400–2500 Myr, such a variation is comparable with a 50–100 °C uncertainty in the temperature at the depth of the mechanical bottom of the mantle lithosphere. The same stress level would completely eliminate the elastic core of the upper crust, because both mechanisms, ductile and brittle weakening, will be invoked, whereas the initial thickness of the competent upper crust is smaller than the thickness of the competent mantle. For younger lithosphere, the influence of horizontal stress is even larger. The typical value of $\bar{\gamma}$ for mantle Alpine lithosphere (Fig. 8) is around 50 MPa, which gives a 4 km decrease of thickness of the competent portion of the mantle lithosphere at the same stress level of 200 MPa. The absolute value of this decrease is less than that induced in the old plate shown in Fig. 6(a), but in relation to the initial mechanical thickness of the mantle lithosphere ($\sim$15–25 km) this gives a larger (20–30 per cent) decrease of the initial mechanical thickness of the mantle lithosphere.

The flexural stresses induced by distributed vertical loads (mountains or slab pull) may essentially reduce the effective mechanical thickness of such pre-weakened lithosphere, sometimes practically to zero, corresponding to the state of local isostasy. Bertotti *et al.* (1996) have found that southern Alpine EET may drop to <5 km at points of greatest flexure (practical slab break-off), whereas the average EET is of the order 20 km (Royden 1993). The effect of an excess normal stress (vertical loading by sediments and topography) is, in fact, two-fold: first, the vertical load increases the local brittle-strength limits due to an increase of the confining pressure (Cloetingh *et al.* 1982); second, inhomogeneously distributed vertical loads cause bending of the lithosphere, and the associated flexural stresses may result in weakening of the lithospheric plate (Burov & Diament 1995). This effect is demonstrated in Fig. 4(b), but see also Section 5.1 and Appendix A. Large mountains and sediment deposits are associated with significant flexural stresses in the underlying lithosphere that result in plate weakening. It has been shown, both from the observations of plate flexure (e.g. Abers & Lyon-Caen 1990), and from theory (Burov & Diament 1992, 1995), that the EET

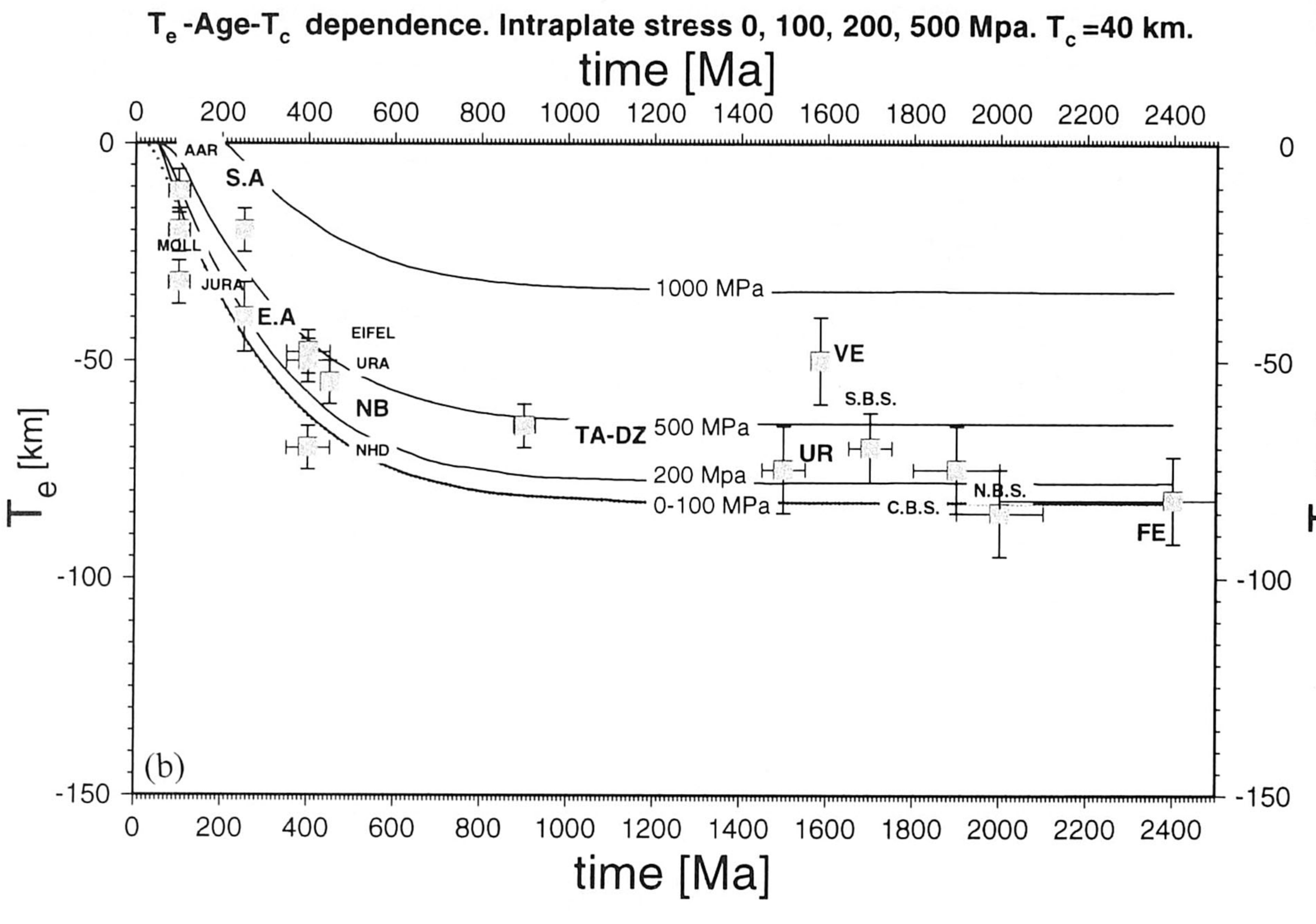

Figure 12. (*Continued.*)

beneath highlands can decrease by 50–80 per cent as compared to the unloaded state of surrounding lowlands. Since the highs of the relief and thickness of sedimentary deposits change with time, the EET will also be subject to temporal changes. On the other hand, since the EET controls plate deflection, and, consequently, topography, topographic relief and EET are interdependent.

5.4 Effect of high horizontal stress (unstable regime of deformation)

If the horizontal stress exceeds a certain limiting value, an unstable buckling or folding of the lithosphere can develop (e.g. Smith 1975, 1977, 1979). At the fixed basic strain rate, the critical stress generally depends on the thickness-to-length ratio of the competent lithospheric layers, and partly on the distribution of the surface loads. This value of the critical stress is about 75–200 MPa for the young lithosphere and about 500 MPa for the old lithosphere. The predominant wavelength of folding is roughly proportional to a factor of 4–6 of the thickness of a competent layer subjected to folding. It is also important to note that the weak lower crust can permit detachment folding of the upper crust and lithospheric mantle. In the case of detachment folding, two dominant wavelengths of the deformation can be observed. These wavelengths can be easily separated, since the upper-crustal folding is not associated with the deformation of density boundaries (in the absence of a strong density contrast on the upper-crust/lower-crust boundary), whereas the mantle folding results in Moho deflection, producing gravity anomalies (Marthinod & Davy 1992; Burov *et al* 1993). There is no significant contribution from the deflection of the upper-crust/lower-crust boundary to the observed gravity anomalies, but only a contribution from the deflection of the lower-crust/mantle boundary (Bouguer anomaly). In the continental areas there are a number of examples of prominent folding, such as the Eurekan fold belt (Stephenson *et al.* 1990; Stephenson & Cloetingh 1991), central Australia (Stephenson & Lambeck 1985), central Asia (Marthinod & Davy 1992; Nikishin *et al.* 1993; Burov *et al.* 1993; Cobold *et al.* 1993), the Tibetan plateau (Burg, Davy & Marthinod 1994) and the Transcontinental Arch of North America (Ziegler *et al.* 1995).

Using analytical expressions relating the dominant wavelength of lithosphere folding and the thickness of the competent layers (e.g. Burov *et al.* 1993), we computed a theoretical relationship between the lithospheric age and the dominant wavelength of folding, for a comparison with existing data (Fig. 14). The results demonstrate a good correlation between the theoretically predicted and the observed wavelength of folding, although in some cases (central Asia, central Australia)

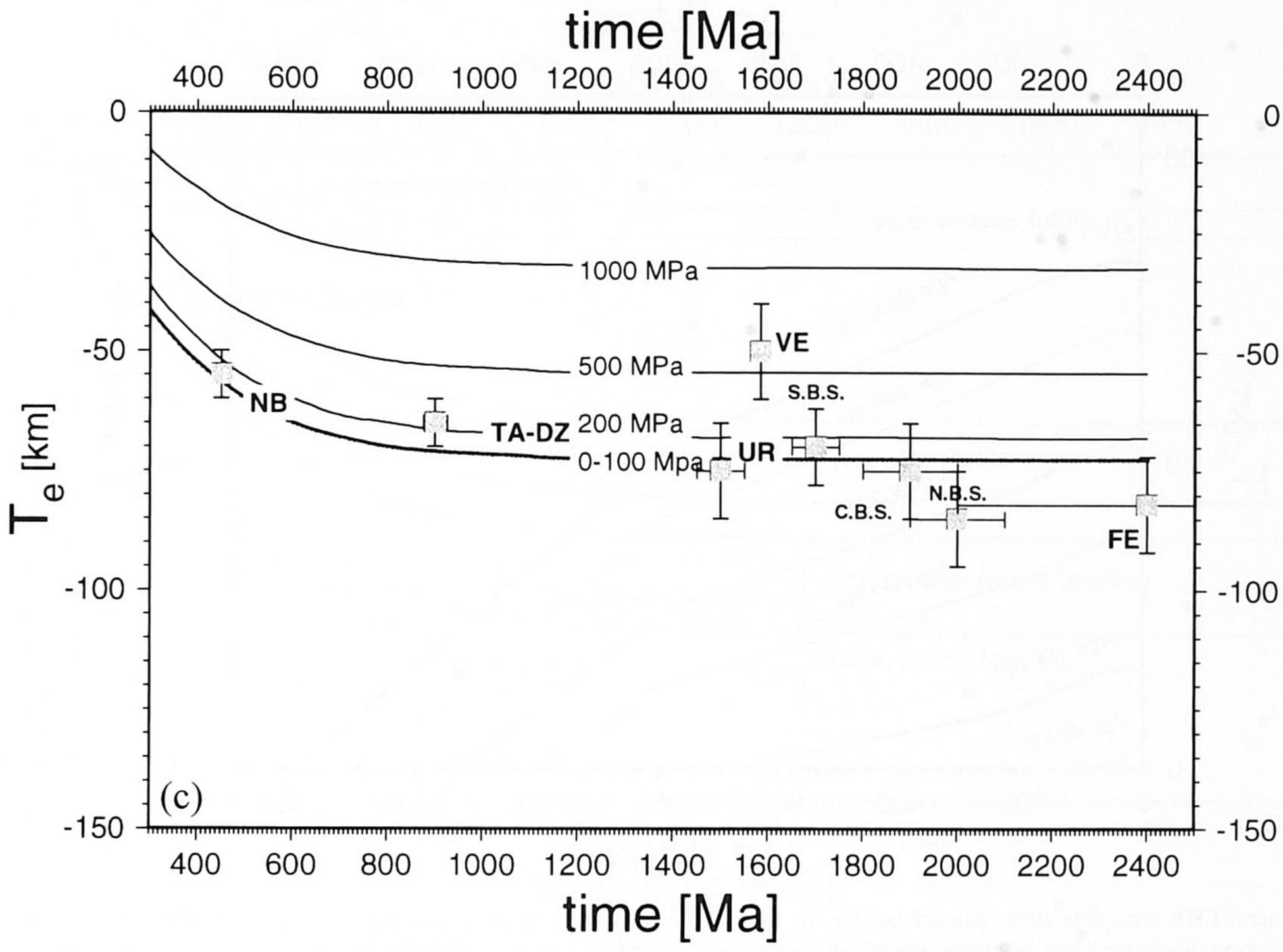

Figure 12. (*Continued.*)

the actual thermal age of the lithosphere is subject to large uncertainties. Although the accurate analytical expressions relating the dominant wavelength of folding with the thickness of the competent layers of the non-Newtonian crust and mantle are quite complex (e.g. Smith 1975, 1977, 1979; Burov *et al.* 1993), an asymptotic relation for a Newtonian rheology and single-layer folding is quite simple (e.g. Turcotte & Schubert 1982):

$$\lambda_d = 2\pi h \left(\frac{1}{6} \frac{\mu_{l1}}{\mu_{l2}} \right)^{1/3}.$$

Here, λ_d is the dominant wavelength of folding, h is the thickness of the corresponding competent layer (crustal or mantle), and μ_{l1} and μ_{l2} are the effective viscosities of the strong layer and weak surrounds, respectively. For the quartz-controlled crust and olivine-controlled mantle, the ratio μ_{l1}/μ_{l2} is of the order of 10^3–10^4, thus meaning that λ_d is ~ 5–$6h$. This estimate is in good agreement with more accurate solutions for non-Newtonian rheologies and with the results of numerical experiments (e.g. Beekman 1994).

6 CONCLUSIONS

Our combined analysis of rheological structures and EET estimates of Europe and Eurasia suggests that EET estimates inferred from rheological and intraplate seismicity data are in good agreement with values obtained from flexural models of these regions. Therefore, it appears that EET estimates can be used to constrain the lithospheric rheology of Europe and Eurasia. Our analysis of variations of EET values shows that most of western and eastern European continental lithosphere has weak lower-crustal rheologies associated with mechanical decoupling between the crust and mantle. Our analysis also suggests the absence of a significant difference in the mechanical behaviour of very old Precambrian lithosphere and middle-aged Variscan lithosphere. This is also consistent with predictions of the plate-cooling model that suggests minor temperature control on EET variations after approximately 400 Ma. Younger Alpine lithosphere exhibits a much stronger EET dependence on age, and a large difference in the mechanical strength supposedly associated with weakening of the lithosphere by flexural and intraplate stresses. The predicted and observed EET values in Alpine Europe support the theory that the mechanical strength of young lithosphere is largely controlled by crustal strength.

The regional horizontal in-plane stress may have a significant effect on the integrated strength of the crust and of the upper mantle, and therefore on the EET. Tectonic stresses of 200–500 MPa, for example, may decrease the EET of middle-aged lithosphere (400 Ma) by 15–20 per cent, but for lithosphere younger than 200 Ma this decrease may be as large as 30 per cent for the same level of stress. The effect of in-plane stresses on the EET also depends on Moho depth, which

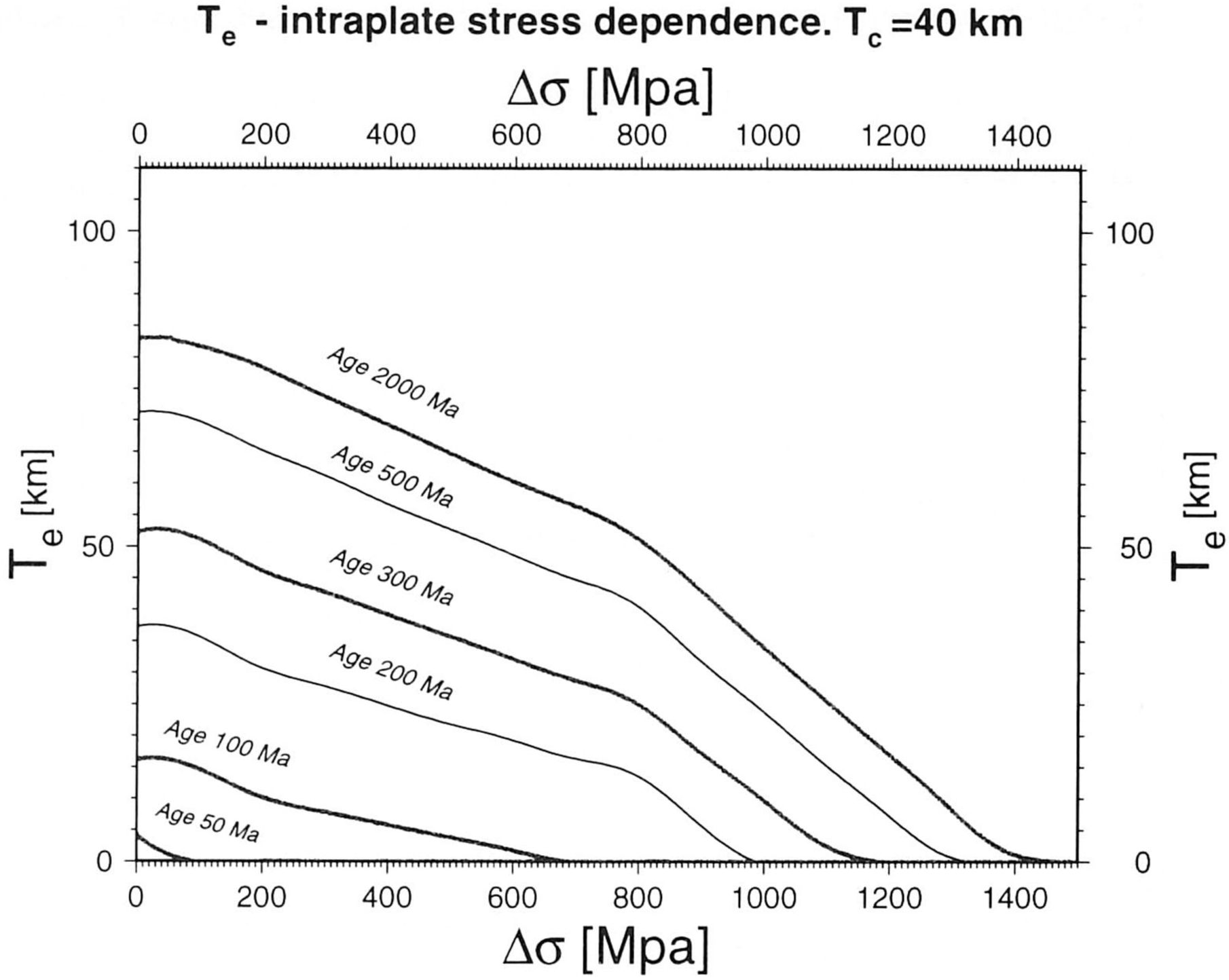

Figure 13. General EET–intraplate stress dependence for the lithosphere with an average crustal thickness of 40 km, for ages 0–2000 Ma. Note that, while the young lithosphere can be almost completely weakened by moderate stresses of 100 MPa, the old lithosphere remains strong even at very high stress levels of 1000 MPa.

controls the thickness of the competent mantle lithosphere (the total mechanical thickness of the lithosphere is mostly dependent on the geotherm, and thus the thickness of the mechanical mantle will be smaller if the crust is thicker). The horizontal stress may facilitate weakening of the lower crust with subsequent crust–mantle decoupling [although for the lithosphere with thick (>35 km) crust and/or low temperature of creep activation in the lower crust such decoupling may be permanent (Burov & Diament 1995)]. The effect of in-plane stresses on average EET is comparable to effects of variation in temperature by from 10–15 per cent for old plates (older than 400 Ma) to 15–20 per cent for young plates (100–250 Ma) and 20–30 per cent for very young plates (~100 Ma). This suggests that the variations in the stress level in Europe's lithosphere might contribute significantly to the observed variations in EET estimates, which so far have been attributed primarily to variations in vertical loading history and temperature.

For higher levels of horizontal stress, the presence of decoupled lithosphere may lead to various spatial scales of lithospheric and crustal folding. Analysis of folding wavelengths from different parts of the planet confirms the inferences made from our study of the mechanical properties of European and Eurasian lithosphere. The wavelength of lithospheric folding appears to be directly related to the thicknesses of the competent crust and mantle. These findings suggest that the dominant wavelength of folding is directly related to EET. The thickness of the competent mantle is generally controlled by the age of the lithosphere, whereas the thickness of the competent crust depends on intrinsic variations in mineralogical composition, content of fluids and melts, and on the concentration of heat-producing elements.

Crust/mantle decoupling can result in a dramatic decrease (by a factor of two or so) of the EET. Comparison of most western European and eastern European data for estimates of the EET with theoretical predictions demonstrates the importance of the crust/mantle decoupling in European and Eurasian lithosphere. Our analysis also supports inferences on lithospheric rheology made on the basis of experimental rheology data, seismic, heat-flow and other geophysical observations. The currently available estimates of EET, therefore, provide independent constraints on the lithospheric rheology of Europe and Eurasia.

ACKNOWLEDGMENTS

This research was partly funded by the International Lithosphere Program. The Institut de Physique du Globe de Paris and the Vrije Universiteit provided excellent computing facilities. EBB was funded through CEA (France). We benefited from constructive rigorous reviews by G. Ranalli and R. Meissner. This is Netherlands Research School of Sedimentary Geology publication number 94.09.09. The IPGP contribution number is 1381 of 19.07.95.

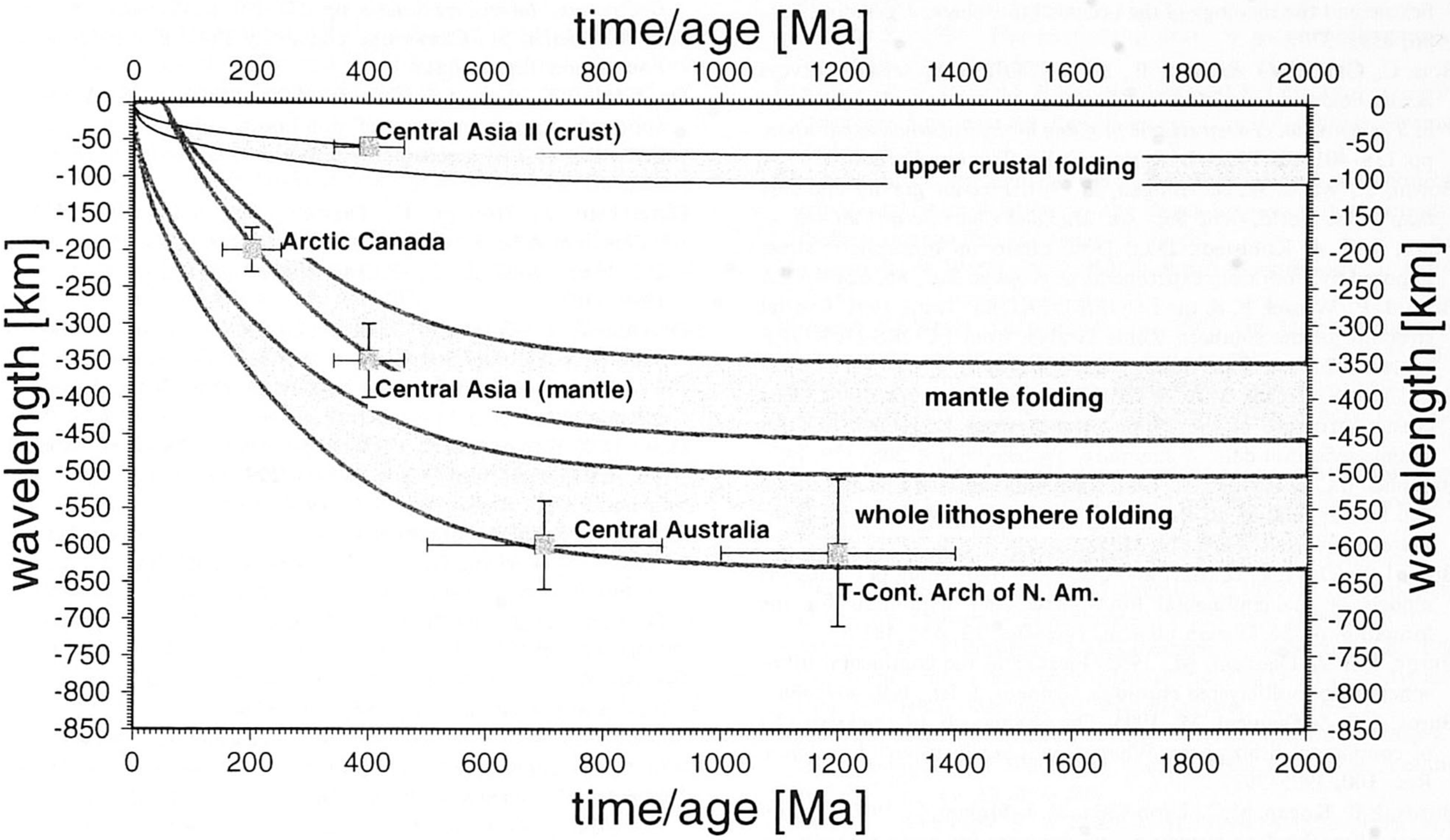

Figure 14. Dependence between the age, MSC, MSL and wavelength of bi-harmonic folding: example of Arctic Canada (young) (Stephenson *et al.* 1990), central Asia (middle age) (Burov *et al.* 1993); Australia (old) (Stephenson & Lambeck 1985) and the Transcontinental Arch of North America (very old) (Ziegler *et al.* 1995). Grey lines: predicted wavelength of folding of the crustal lithosphere, mantle lithosphere and for the whole-lithosphere folding. Squares correspond to the direct estimates. The shaded bands correspond to the depth intervals bounding possible variations in the wavelength of folding for the given age. These variations are associated with the uncertainties in the mechanical thickness of the competent layers (Fig. 10) and with the change of this thickness due to horizontal stress (Figs 11–13).

REFERENCES

Abers, A.G. & Lyon-Caen, H., 1990. Regional gravity anomalies, depth of the foreland basin and isostatic compensation of the new Guinea highlands, *Tectonics,* **9,** 1479–1493.

Adamia, Sh.A., Lordkipanidze, M.B. & Zakaridze, G.S., 1977. Evolution of an active continental margin as exemplified by the Alpine history of the Caucasus, *Tectonophysics,* **40,** 183–199.

Artemjev, E.M. & Kaban, M.K., 1994. Density inhomogeneities, isostasy and flexural rigidity of the lithosphere in the Transcaspian region, *Tectonophysics,* **240,** 281–297.

Artemjev, E.M., Belov, A.P., Kaban, M.K. & Karaev, A.I., 1972a. Isotasiya lithospheri Turkmenii. (Isostasy of the lithosphere in Turkmenia), *Geotektonika,* **1,** 68–83.

Artemjev, E.M., Gordin, V.M. & Kucherinenko, V.A., 1992b. Spektralno-statistichesky analiz anomal'nogo gravitazionnogo polya (Spectral-Statistical analysis of the anomalous gravity field of Eurasia), *Dokl. Acad. Nauk SSSR,* **325(4),** 607–703.

Artemjev, E.M., Kaban, M.K., Kucherinenko, V.A., Demyanov, G.V. & Taranov, V.A., 1994. Subcrustal density inhomogeneities of Northern Eurasia as derived from the gravity data and isostatic models of the lithosphere, *Tectonophysics,* **240,** 249–280.

Austrheim, H., 1994. Eclogitization of the deep crust in continent collision zones, *C. R. Acad. Sci. Paris, t. 319, serie II,* 761–774.

Babaev, A.M., Koshlakov, G.V. & Mirzoev, K.M., 1978. Seismic regionalization of Tadjikistan, Donish, Dushanve (in Russian).

Balling, N., 1992. BABEL seismic profiles across the southern Baltic Shield and the Tornquist Zone, in The BABEL Project, Commission of the European Communities, Directorate General XII, Science, Research and Development, Belgium, R&D Program Non-Nuclear Energy Area: Deep Reservoir Geology, pp. 141–146, eds Meissner, R., Snyder, D., Balling, N. & Staroste, E.

Banda, E. & Cloetingh, S., 1992. Physical properties of the Europe's lithosphere, in *A continent revealed: The European Geotraverse,* pp. 71–80, eds Blundell, D., Freeman R. & Mueller, S. Cambridge Univ. Press/European Science Foundation, Cambridge.

Beaumont, C. & Quinlan, G., 1994. A geodynamic framework for interpreting crustal scale seismic reflectivity patterns, *Geophys. J. Int.,* **116,** 754–783.

Beekman, F., 1994. Tectonic modelling of thick-skinned compressional intraplate deformation, *PhD thesis,* Free University, Amsterdam.

Belyayevsky, N.A., 1974. The Earth's Crust within the Territory of the USSR (in Russian), Nedra, Moscow.

Benedetti L., 1993. *Bilan mécanique d'une orogenèse active: le Tien Shan, Rapport de stage effectue dans le laboratoire de tectonique et mechanique de la lithosphère,* IPGP, Paris.

Bertotti, G., Picotti, V., Bernoulli, D. & Castellarin, A., 1993. From rifting to drifting: tectonic evolution of the South-Alpine upper crust from the Triassic to the Early Cretaceous, *Sedimentary Geology,* **86,** 53–76.

Bertotti, G., ter Voorde, M., Picotti, V. & Cloetingh, S., 1996. Flexure-induced lithospheric weakening and the role of inherited crustal heterogeneities: $2\frac{1}{2}$-D evolution of the South-Alpine foredeep, *Tectonics,* submitted.

Blundell, D., Freeman R. & Mueller, S., eds, 1992. *A continent revealed: The European Geotraverse,* Cambridge University Press/European Science Foundation, Cambridge.

Bodine, J.H., Steckler, M.S. & Watts, A.B., 1981. Observations of flexure and the rheology of the oceanic lithosphere, *J. geophys. Res.,* **86,** 3595–3707.

Bois, C., Gabriel, O. & Pinet, B., 1990. ECORS deep seismic surveys across Paleozoic and Mesozoic basins in France and adjacent areas, in *The potential of deep seismic profiling for hydrocarbon exploration,* pp. 138–401, eds Pinet, B. & Bois, C. Ed. Technip, Paris.

Bowin, C., Warsi, W. & Milligan, J., 1981. Free-air gravity anomaly map of the world, *Geol. Soc. Am. Map and Chart Series,* MC-46.

Brace, W.F. & Kohlstedt, D.L., 1980. Limits on lithospheric stress imposed by laboratory experiments. *J. geophys. Res.,* **85,** 6248–6252.

Brun, J.-P., Wenzel, F. & the ECORS-DEKORP Team, 1991. Crustal structure of the southern Rhine Graben from ECORS-DEKORP seismic reflection data, *Geology,* **19,** 758–762.

Brun, J.-P., Gutscher, M.A. & DEKORP-ECORS teams, 1992. Deep crustal structure of the Rhine Graben from DEKORP-ECORS seismic reflection data: A summary, *Tectonophysics,* **208,** 139–147.

Burchfiel, B.C. & Royden, L., 1982. Carpathian forland fold and thrust belt and its relation to Pannonian and others basins, *Amer. Assoc. Petrol. Geol. Bull.,* **66,** 1179–1195.

Burg, J.-P., Davy, P. & Marthinod, J., 1994. Shortening of analogous models of the continental lithosphere: New hypothesis for the formation of the Tibetan plateau, *Tectonics,* **13,** 475–483.

Burov, E.B. & Diament, M., 1992. Flexure of the continental lithosphere with multilayered rheology, *Geophys. J. Int.,* **109,** 449–468.

Burov, E.B. & Diament, M., 1995. The effective elastic thickness (T_e) of continental lithosphere: What does it really mean? *J. geophys. Res.,* **100,** 3905–3927.

Burov, E.B., Kogan, M.G., Lyon-Caen, H. & Molnar, P., 1990. Gravity anomalies, the deep structure, and dynamic processes beneath the Tien Shan, *Earth planet. Sci. Lett.,* **96,** 367–383.

Burov, E.B., Lobkovsky, L.I., Cloetingh, S. & Nikishin, A.M., 1993. Continental lithosphere folding in Central Asia (part 2), constraints from gravity and topography, *Tectonophysics,* **226,** 73–87.

Burov, E.B., Houdry, F., Diament M. & Deverchere, J., 1994. A broken plate beneath the North Baikal rift zone revealed by gravity modelling, *Geophys. Res. Lett.,* **21,** 129–132.

Burtman, V.S., 1975. Structural geology of the Variscan Tien Shan, USSR, *Am. J. Sci.,* **272A,** 157–186.

Byerlee, J.D., 1978. Friction of rocks, *Pure appl. Geophys.,* **116,** 615–626.

Carter, N.L. & Tsenn, M.C., 1987. Flow properties of continental lithosphere, *Tectonophysics,* **36,** 27–63.

Chen, W.-P. & Molnar, P., 1983. Focal depths of intracontinental and intraplate earthquakes and their implications for the thermal and mechanical properties of the lithosphere, *J. geophys. Res.,* **88,** 4183–4214.

Cloetingh, S, & Banda, E., 1992. Europe's lithosphere—physical properties. Mechanical structure, in *A continent revealed: The European Geotraverse,* pp. 80–91, eds Blundell, D., Freeman R. & Mueller, S., Cambridge University Press/European Science Foundation, Cambridge.

Cloetingh, S.A.P.L., Wortel, M.J.R. & Vlaar, N.J., 1982. Evolution of passive continental margins and initiation of subduction zones, *Nature,* **297,** 139–142.

Cloetingh, S., van der Beek, P.A., van Rees, D., Roep, Th.B., Bierman, C. & Stephenson, R.A., 1992. Flexural interaction and the dynamics of Neogene extensional basin formation in the Alboran-Betic region, *Geo-Marine Lett.,* **12,** 66–75.

Cobold, P.R., Davy, P., Gapais, D., Rossello, E.A., Sadybakasov, E., Thomas, J.C., Tondji Biyo, J.J. & de Urreiztieta, M., 1993. Sedimentary basins and crustal thickening, *Sedimentary Geology,* **86,** 77–89.

Cochran, J.R., 1980. Some remarks on isostasy and the long-term behavior of the continental lithosphere, *Earth planet. Sci. Lett.,* **46,** 266–274.

Deichmann, N. & Baer, M., 1990. Earthquake focal depth below the Alps and northern Alpine foreland of Switzerland, in *The European Geotraverse: Integrative Studies,* pp. 277–288, eds Freeman, R., Giese, P. & Mueller, St., Cambridge University Press/European Science Foundation, Cambridge.

De Rito, R.F., Cozzarelli F.A. & Hodge, D.S., 1986. A forward approach to the problem of non-linear viscoelasticity and the thickness of the mechanical lithosphere, *J. geophys. Res.,* **91,** 8295–8313.

Deverchere, J., Houdry, F., Diament, M., Solonenko, N.V. & Solonenko, A.V., 1991. Evidence for a seismogenic upper mantle and lower crust in the Baikal rift, *Geophys. Res. Letters,* **18,** 1099–1102.

Deverchere, J., Houdry, F., Solonenko, N.V., Solonenko, A.V. & Sankov, V.A., 1993. Seismicity, active faults and stress field of the North Muya Region, Baikal Rift: New insights on the rheology of extended continental lithosphere, *J. geophys. Res.,* **98,** 19 895–19 912.

Doser D. & Yarwood, D.R., 1994. Deep crustal earthquakes associated with continental rifts, *Tectonophysics,* **229,** 123–131.

England, P.C. & Richardson, S.W., 1980. Erosion and the age dependence of continental heat flow, *Geophys. J. R. Astr. Soc.,* **62,** 421–437.

EUGENO-S Working Group, 1988. Crustal structure and tectonic evolution of the transition between the Baltic Shield and the North German Caledonites (the EUGENO-S Project), *Tectonophysics,* **150,** 253–348.

Forsyth, W., 1980. Comparison of mechanical models of the oceanic lithosphere, *J. geophys. Res.,* **85,** 6364–6368.

Franke, W., 1992. Phanerozoic structures and events in Central Europe, in *A continent revealed: The European Geotraverse,* pp. 164–180, eds Blundell, D., Freeman, R. & Mueller, S., Cambridge University Press/European Science Foundation, Cambridge.

Fuchs, K., Bonjer, K.-P., Gajewski, D., Luschen, E., Prodehl C., Sandmeier, K.J., Wenzel, F. & Wilhelm, H., 1987. Crustal evolution of the Rhinegraben area, I. Exploring the lower crust in the Rhinegraben rift by unified geophysical experiments, *Tectonophysics,* **141,** 261–275.

GEODAS CD-ROM, 1992. *Alpha Release,* US Dept. of Commerce, NGDC, NOAA.

Govers, R., Wortel, M.J.R., Cloetingh, S.A.P.L. & Stein, C.A., 1992. Stress magnitude estimates from earthquakes in oceanic plate interiors, *J. geophys. Res.,* **97,** 11 749–11 759.

Hamilton, W., 1970. The Uralides and the motion of the Russian and Siberian platforms, *Geol. Soc. Am. Bull.,* **81,** 2553–2576.

Hendrix, M.S., Trevor, A.D. & Graham, S.A., 1994. Late Oligocene–early Miocene unroofing in the Chinese Tien Shan: An early effect of the India-Asia collision, *Geology,* **22,** 487–490.

Henkel, H., Lee, M.K., Lund, C.-E. & Rasmussen, T., 1990. An integrated geophysical interpretation of the 2000 km FENNOLORA section of the Baltic Shield. in *The European Geotraverse: Itegrative studies,* pp. 1–47, eds Freeman, R., Giese, P. & Mueller, St., European Science Foundation, Strasbourg, France.

Horváth, F., 1993. Toward a mechanical model for the formation of the Pannonian basin, *Tectonophysics,* **226,** 333–357.

Karner, G.D. & Watts, A.B., 1983. Gravity anomalies and flexure of the lithosphere at mountain ranges, *J. geophys. Res.,* **88,** 10 449–10 477.

Karner, G.D., Steckler, M.S. & Thorne, J.A., 1983. Long-term thermomechanical properties of the continental lithosphere, *Nature,* **304,** 250–253.

Kirby, S.H., 1983. Rheology of the lithosphere. *Rev. Geophys.,* **21,** 1458–1487.

Kirby, S.H. & Kronenberg, A.K., 1987a. Rheology of the lithosphere: Selected topics, *Rev. Geophys.,* **25,** 1219–1244.

Kirby, S.H. & Kronenberg, A.K., 1987b. Correction to 'Rheology of the lithosphere: Selected topics', *Rev. Geophys.,* **25,** 1680–1681.

Kirby, S.H., Durham, W.B. & Stern, L.A., 1991. Mantle phase changes

and deep-earthquake faulting in subducting lithosphere, *Science,* **252,** 216–224.

Klemperer, S. & Hobbs, R., 1991. *The BIRPS Atlas, deep seismic reflection profiles around the British Isles,* Cambridge University Press, Cambridge.

Kogan, M.G. & McNutt, M., 1986. Isostasy in USSR, 1: Admittance Data, in *Composition, Structure, and Dynamics of the Lithosphere–Asthenosphere system,* pp. 65–77, eds Fuchs, K., Froidevaux, C., AGU, Washington, DC.

Kruse, S. & McNutt, M., 1988. Compensation of Paleozoic orogens: a comparison of the Urals to the Appalachians, *Tectonophysics,* **154,** 1–17.

Kruse, S. & Royden, L., 1994. Bending and unbending of an elastic lithosphere: The Cenozoic history of the Apennine and Dinaride fordeep basins, *Tectonics,* **13,** 278–302.

Kunin, N.Ya., Sheih-Zade, E.R. & Semenova, G.I., 1992. Stroenie litosferi Evrazii (Structure of the Eurasian lithosphere.), Mezhduvedomstvennii Geofiz, Komitet Rossiiskoi Akademii Nauk, Moscow (in Russian).

Kusznir, N.J., 1991. The distribution of stress with depth in the lithosphere: thermo-rheological and geodynamic constraints, *Phil. Trans. R. Soc. Lond.,* A **337,** 95–110.

Kusznir, N.J. & Karner, G., 1985. Dependence of the flexural rigidity of the continental lithosphere on rheology and temperature, *Nature,* **316,** 138–142.

Kusznir, N.J. & Park, R.G., 1987. The extensional strength of the continental lithosphere: its dependence on geothermal gradient, and crustal composition and thickness, in: Continental Extensional Tectonics, eds Coward, M.P., Dewey, J.F. & Hancock, P.L., *Geol. Soc. London Spec. Publ.,* **28,** 35–52.

Kusznir, N.J. & Matthews, D.H., 1988. Deep seismic reflections and the deformational mechanics of the continental lithosphere, *J. Petrol.,* 63–87.

Lobkovsky, L.I., 1988. *Geodynamics of Spreading and Subduction zones, and the two-level plate tectonics,* Nauka, Moscow (in Russian).

Lobkovsky, L.I. & Kerchman, V.I., 1992. A two-level concept of plate tectonics: application to geodynamics, *Tectonophysics,* **199,** 343–374.

Lyon-Caen, H. & Molnar, P., 1983. Constraints on the structure of the Himalaya from an analysis of gravity anomalies and a flexural model of the lithosphere, *J. geophys. Res.,* **88,** 8171–8191.

Lyon-Caen, H. & Molnar, P., 1984. Gravity anomalies and the structure of the western Tibet and the southern Tarim basin, *Geophys. Res. Lett.,* **11,** 1251–1254.

Ma, X., 1987a. *Lithospheric dynamic Atlas of China,* China Cartographic Publishing House, Beijing.

Ma, X., 1987b. *Lithospheric dynamic map of China and adjacent seas with explanatory notes,* scale 1:4,000,000, Geological Publishing House, Beijing.

Mackwell, S.J., Bai, Q. & Kohlstedt, D.L., 1990. Rheology of olivine and the strength of the lithosphere, *Geophys. Res. Lett.,* **17,** 9–12.

Marquis, G., Jones, A.G. & Hyndman, R.D., 1995. Coincident conductive and reflective middle and lower crust in southern British Columbia, *Geophys. J. Int.,* **120,** 111–131.

Marthinod, J. & Davy, Ph., 1992. Periodic instabilities during compression or extension of the lithosphere: 1. Deformation modes from an analytical perturbation method, *J. geophys. Res.,* **97,** 1999–2014.

Matencu, L., Zoetemeijer, R., Cloetingh, S. & Dinu C., 1994. Tectonic modelling of the Getic depression, *ALCAPA II workshop,* Program and abstracts, 12.

McAdoo, D.C., Martin, C.F. & Polouse, S., 1985. Seasat observations of flexure: evidence for a strong lithosphere, *Tectonophysics,* **116,** 209–222.

McNutt, M., 1980. Implications of regional gravity for state of stress in the Earth's crust and upper mantle, *J geophys. Res,* **85,** 6377–6396.

McNutt, M. & Kogan, M.G., 1986. Isostasy in USSR, 2: Interpretation of admittance data, in *Composition, Structure, and Dynamics of the Lithosphere–Asthenosphere system,* pp. 78–83, eds Fuchs, K. & Froidevaux, C., AGU, Washington DC.

McNutt, M. & Kogan, M.G., 1987. Isostasy in USSR 1: Admittance Data, *AGU Trans.,* 301–307.

McNutt, M., Diament, M. & Kogan, M.G., 1988. Variations of elastic plate thickness at continental thrust belts, *J. geophys. Res.,* **93,** 8825–8838.

Meissner, R., 1986. *The continental crust, a geophysical approach,* Academic Press, London.

Meissner, R. & Bortfeld, R.K., eds, 1990. *DEKORP-Atlas, results of Deutsches Kontinentales Reflexionsseismisches Programm,* Springer Verlag, Berlin.

Meissner, R. & Strehlau, J., 1982. Limits of stresses in continental crusts and their relation to the depth-frequency distribution of shallow earthquakes, *Tectonics,* **1,** 73–89.

Meissner, R. & Wever, Th., 1988. Lithospheric rheology, *J. Petrol.,* 53–61.

Meissner, R., Wever, Th. & Flüh, E.R., 1987. The Moho in Europe—implications of crust development, *Ann. Geophys., Ser.* B., **5,** 357–364.

Morley, C.K., 1989. Extension, detachment, and sedimentation in continental rifts (with particular reference to East Africa), *Tectonics,* **8,** 1175–1192.

Morner, N.-A., 1990. Glacial isostasy and long-term crustal movements in Fennoscandia with respect to lithospheric and asthenospheric processes and properties, *Tectonophysics,* **176,** 13–24.

Müller, B., Zoback, M.L., Fuchs, K., Mastin, L., Gregersen, S., Pavoni, N., Stephansson, O. & Lunggren, C., 1992. Regional patterns of stress in Europe, *J. geophys. Res.,* **97,** 11 783–11 803.

Nikishin, A.M., Lobkovsky, L.I., Cloetingh, S. & Burov, E.B., 1993. Continental lithosphere folding in Central Asia (Part 2): constraints from geological observations, *Tectonophysics,* **226,** 59–72.

Okay, A.I., Sengör, A.M.C. & Görür, N., 1994. Kinematic history of the opening of the Black Sea and its effect on the surrounding regions, *Geology,* **22,** 267–270.

Okaya, N., Cloetingh, S. & Mueller, St., 1996. A lithospheric cross section along the European Geotraverse through the Swiss Alps—an example of continent-continent collision (part II): aspects of the present-day mechanical structure, *Geophys. J., Int.,* submitted.

Parsons, B. & Sclater, J.G., 1977. An analysis of the thermal structure of the plates, *J geophys. Res.,* **82,** 803–827.

Peper, T. & Cloetingh, S., 1992. Lithosphere dynamics and tectonostratigraphic evolution of the Mesozoic Betic rifted margin (southeastern Spain), *Tectonophysics,* **203,** 345–361.

Pfiffner, A., 1992. Alpine Orogeny, in *A continent revealed: The European Geotraverse,* pp. 180–190, eds Blundell, D., Freeman, R. & Mueller, S., Cambridge University Press/European Science Foundation, Cambridge.

Philippot, P., 1987. 'Crack seal' vein geometry in eclogitic rocks, *Geodinamica Acta (Paris),* **1,** 171–181.

Philippot, P., 1993. Fluid-melt-rock interaction in mafic eclogites and coesite-bearing metasediments: constraints on volatile recycling during subduction, *Chem. Geol.,* **108,** 93–112.

Plyusnin, K.P., 1963. Tectonic zoning of the central and southern Urals, *Doklady Acad. SCI. USSR, Earth Sci. Sec.,* **152,** 92–94.

Ranalli, G., 1987. *Rheology of the Earth. Deformation and flow processes in geophysics and geodynamics,* Allen & Unwin, Boston.

Ranalli, G., 1994. Nonlinear flexure and equivalent mechanical thickness of the lithosphere, *Tectonophysics,* **240,** 107–114.

Ranalli, G., 1995. *Rheology of the Earth,* 2nd edn, Chapman & Hall, London.

Ranalli, G. & Murphy, D.C., 1987. Rheological Stratification of the Lithosphere, *Tectonophysics,* **132,** 281–295.

Rapp, R.H. & Pavlis, N.K., 1990. The development and analyses of geopotential coefficient models, to spherical harmonic degree 360, *J. geophys. Res.,* **95,** 21 885–21 911.

Robinson, A., Spadini, G., Cloetingh, S. & Rudat, J., 1995. Stratigraphic evolution of the Black sea: inferences from basin modelling, *Marine and Petroleum Geology,* **12,** 821–835.

Royden, L.H., 1993. The tectonic expression slab pull at continental convergent boundaries, *Tectonics,* **12,** 303–325.

Royden, L. & Karner, G.D., 1984. Flexure of the continental lithosphere beneath the Apennine and Carpathian fordeep basins: Evidence for an insufficient topographic load, *Am. Assoc. Petrol. Geol. Bull.*, **68,** 704–712.

Roure, F., Heitzmann, P. & Polino, R., eds, 1990. Deep structure of the Alps, *Mém. Soc. géol. France, N.S.*, **156.**

Ruppel, C.D., 1992. Thermal structure, compensation mechanisms, and tectonics of actively deforming continents: Baikal rift zone and large scale overthrust and extensional terrains, *PhD thesis,* Mas. Inst. of Technology.

Sclater, J.G., Parsons, B. & Jaupart, C., 1981. Oceans and continents: Similarities and differences in mechanisms of heat loss, *J. geophys. Res.*, **86,** 11 535–11 532.

Sengör, A.M.C., Altiner, D., Cin, A., Üstaomer, T. & Hsü, K.J., 1988. Origin and assembly of the Tethyside orogenic collage at the expense of Gondwanaleand, in Gondwana and Tethys, eds Audley-Charles, M.G. & Hallam, A., *Geol. Soc. Spec. Pub.*, **37,** 119–181.

Seno, T. & Seito, A., 1994. Recent East African earthquakes in the lower crust, *Earth planet. Sci. Lett.*, **121,** 125–135.

Sheffels, B. & McNutt, M., 1986. Role of subsurface loads and regional compensation in the isostatic balance of the Transverse Ranges, California: Evidence of intracontinental subduction, *J. geophys. Res.*, **91,** 6419–6431.

Shudofsky, G.N., 1985. Source mechanisms and focal depths of east African earthquakes using Rayleigh-wave inversion and bodywave modelling, *Geophys. J. R. astr. Soc.*, **83,** 563–614.

Shudofsky, G.N., Cloetingh, S., Stein, S. & Wortel, R., 1987. Unusually deep earthquakes in east Africa: constraints on the thermo-mechanical structure of a continental rift system, *Geophys. Res. Lett.*, **14,** 741–744.

Sibson, R.H., 1980. Transient discontinuities in ductile shear zones, *J. Struct. Geol.*, **2,** 165–171.

Sibson, R.H., 1982. Fault zone models, heat flow, and the depth distribution of earthquakes in the continental crust of the United States, *Bull. seism. Soc. Am.*, **72,** 151–163.

Sokolov, V.B., 1992. Crustal structure of the Urals, *Geotectonics,* **26,** 357–366.

Smirnov, Ya.B., 1980. Karti teplovih potokov i glubinnih temperatur territorii SSSR, 1 : 1000000 (Heat flow and abyssal temperature maps of the USSR territory, scale 1 : 1000000), Glavnoye Upravlenie Geodezii i Kartografii pri Sovete Ministrov SSSR, Moskva (in Russian).

Smith, R.B., 1975. Unified theory of the onset of folding, boudinage and mullion structure, *Geol. Soc. Am. Bull.*, **88,** 1601–1609.

Smith, R.B., 1977. Formation of folds, boudinage and mullions non-Newtonian materials, *Geol. Soc. Am. Bull.*, **88,** 312–320.

Smith, R.B., 1979. The folding of a strongly non-Newtonian layer, *Am. J. Sci.*, **79,** 272–287.

Stakhovskaya, R.Y. & Kogan, M.G., 1993. Gravity and mechanical modelling of the lithosphere plate's interaction: the regions of Urals and Caucasus, *Abstr. Suppl. No 1 to Terra Nova, 5, EUG VII Strasbourg,* C09-65, 269.

Stephenson, R.A. & Cloetingh, S., 1991. Some examples and mechanical aspects of continental lithospheric folding, *Tectonophysics,* **188,** 27–37.

Stephenson, R.A., Ricketts, B.D., Cloetingh, S.A., Beekman, F., 1990. Lithosphere folds in the Eurekan orogen, Arctic Canada?, *Geology,* **18,** 603–606.

Stephenson, R. & Lambeck, K., 1985. Isostatic response of the lithosphere with in-plane stress: application to Central Australia, *J. geophys. Res.*, **90,** 8581–8588.

Timoshenko, S.P. & Woinowsky-Krieger, S., 1959. *Theory of Plates and Shells,* McGraw-Hill, New York, NY.

Tse, S.T. & Rice, J.R., 1986. Crustal earthquake instability in relation to the depth variation of friction slip properties, *J. geophys. Res.*, **91,** 9452–9472.

Tsenn, M.C. & Carter, N.L., 1987. Flow properties of continental lithosphere, *Tectonophysics,* **136,** 27–63.

Turcotte, D.L. & Schubert, G., 1982. *Geodynamics. Applications of continuum physics to geological problems,* J. Wiley & Sons, New York, NY.

van der Beek, P.A. & Cloetingh, S., 1992. Lithospheric flexure and the tectonic evolution of the Betic Cordilleras (SE Spain), *Tectonophysics,* **203,** 325–344.

Volvovksy, B.S. & Volvovsky, I.S., 1975. Razrezi zemnoi kori territorii SSSR po dannim glubinnogo seismicheskogo zondirovaniya (Earth crust cross-sections of the USSR territory according to the deep seismic sounding data), Nauka, Moscow (in Russian).

Vyskocil, V., Burda, M. & Plancar, J., 1983. On the manifestation of shallow and deep density inhomogeneities in the gravity field of the Carpathians, *Geologicky Zbornik, Geologica Carpathica,* **34,** 429–438.

Watts, A.B., 1978. An analysis of isostasy in the world's oceans: 1. Hawaiian-Emperor Seamount Chain, *J. geophys. Res.*, **83,** 5989–6004.

Watts, A.B., 1992. The effective elastic thickness of the lithosphere and the evolution of foreland basins, *Basin Research,* **4,** 169–178.

Watts, A.B. & Talwani, M., 1974. Gravity anomalies seaward of deep-sea trenches and their tectonic implications, *Geophys. J. R. astr. Soc.*, **36,** 57–90.

Watts, A.B. & Torne, M., 1992. Crustal structure and the mechanical properties of extended continental lithosphere in the Valencia through (western Mediterranean), *J. geol. Soc. Lond.*, **149,** 813–827.

Watts, A.B., Bodine J.H. & Steckler, M.S., 1980a. Observations of flexure and the state of stress in the oceanic lithosphere, *J. geophys. Res.*, **85,** 6369–6376.

Watts, A.B., Bodine, J.H. & Ribe, N.M., 1980b. Observation of flexure and the geological evolution of the Pacific Ocean Basin, *Nature,* **283,** 532–537.

Walcott, R.I., 1970. Flexural rigidity, thickness and viscosity of the lithosphere, *J. geophys. Res.*, **75,** 3941–3954.

Wessel, P., 1993. A re-examination of the flexural deformation beneath the Hawaiian islands, *J. geophys. Res.*, **98,** 12 177–12 190.

Wever, T., 1989. The Conrad discontinuity and the top of the reflective lower crust—Do they coincide?, *Tectonophysics,* **157,** 39–58.

Wiens, D.A. & Stein, S., 1983. Age dependence of oceanic intraplate seismicity and implications for lithospheric evolution, *J. geophys. Res.*, **88,** 6455–6468.

Windley, B., 1992. Precambrian Europe, in *A continent revealed: The European Geotraverse,* pp. 139–152, eds Blundell, D., Freeman, R. & Mueller, S., Cambridge University Press/European Science Foundation, Cambridge.

Ziegler, P.A., Cloetingh, S. & van Wees, J.D., 1995. Dynamics of intra-plate compressional deformation: the Alpine foreland and other examples, *Tectonophysics,* **252,** 7–59.

Zielhuis, A. & Nolet, G., 1994. Deep seismic expression of an ancient plate boundary in Europe, *Science,* **265,** 79–81.

Zoback, M.D. *et al.*, 1993. Upper-crustal strength inferred from stress measurements to 6 km depth in the KTB borehole, *Nature*, **365,** 633–635.

Zoetemeijer, R., Desegaulx, P., Cloetingh, S., Roure, F. & Moretti, I., 1990. Lithospheric Dynamics and Tectonic-Stratigraphic evolution of the Ebro Basin, *J. geophys. Res.*, **95,** 2701–2711.

Zoetemeijer, R., Tomek, Č. & Matencu, L., 1994. Flexural modelling of the Outer Carpathians. *EUROPROBE workshop 'PANCARDI', Program and abstracts,* **13.**

Zuber, M.T., 1987. Compression of oceanic lithosphere: an analysis of intraplate deformation in the Central Indian Basin, *J. geophys. Res.*, **92,** 4817–4825.

APPENDIX A: EET AND RHEOLOGY

For a plate infinite in the z-direction, the strain component ε_{zz} along the z-axis normal to the xy-plane, is zero ($\varepsilon_{zz} = 0$). For this case, the bending moment $M = M_x$, horizontal (longitudi-

nal) force component T_x and vertical (shearing) force component F_x per unit width of the plate can be expressed as follows (Burov & Diament 1995):

$$\begin{cases} M_x = -\sum_{i=1}^{n} \int_{y_i^-(\phi)}^{y_i^+(\phi)} \sigma_{xx}(x, y) y_i^*(\phi)\, dy, \\ T_x = -\sum_{i=1}^{n} \int_{y_i^-(\phi)}^{y_i^+(\phi)} \sigma_{xx}(x, y)\, dy, \\ F_x = -\sum_{i=1}^{n} \int_{y_i^-(\phi)}^{y_i^+(\phi)} \sigma_{xy}(x, y)\, dy = \dfrac{\partial M_x}{\partial x}, \end{cases} \tag{A1}$$

where $w = w(x)$ is the vertical deflection of the plate, $\phi \equiv \{x, y, w, w', w''\}$, $y_i^* = y - y_{ri}(\phi)$, y_{ri} is the depth to the neutral plane of the ith elastic core of the plate with multilayered rheology; $y_i^-(\phi) = y_i^-$, $y_i^+(\phi) = y_i^+$ are the depths to the lower and upper low-strength interfaces, and thus $y_i^+ - y_i^- = \Delta h_i(\phi)$ is the thickness of the ith detached layer. The upper limit of integration h_n ($h_n = h_2$ in the case of weak lower crust) corresponds to the depth at which the longitudinal stress σ_{xx} and shear stress σ_{xy} become negligible:

$$\lim_{y \to h_2} \sigma_{xx}, \sigma_{xy} = 0.$$

The equation of static equilibrium of a *thin* plate (Timoshenko & Woinowsky-Krieger 1959), compatible with eq. (A1), is rheology-independent, and thus holds for elastic, plastic, viscous, ductile and mixed rheologies:

$$-\frac{\partial^2 M_x}{\partial x^2} + \frac{\partial}{\partial x}\left(T_x \frac{\partial w}{\partial x}\right) + p_- = p_+, \tag{A2}$$

where

$$p_- = g \int_{h_2}^{h_2 + w(x)} \rho_m(x, y)\, dy - g \int_{h_c}^{h_c + w(x)} \rho_c(x, y)\, dy$$

is the restoring force per unit area; $\rho_m(x, y)$ and $\rho_c(x, y)$ are the densities of the mantle and crustal material, respectively; g is the acceleration due to gravity; and h_c is the thickness of the crust. p_+ is the additional vertical force, equal to the sum of topography loads and effective vertical forces $f_a(x)$ associated with plate-boundary forces:

$$p_+ = g \int_0^h \rho_s(x, y)\, dy + f_a(x),$$

where $h = h(x)$ is the topography elevation and $\rho_s(x, y)$ is the density of the material above the reference sea-level.

In the case of the inelastic rheology (eqs 2.1, 2.2), eq. (A2) is non-linear because the moment M_x and the longitudinal force T_x are functions of plate deflection w and its derivatives w', w'' ... (Burov & Diament 1992).

To estimate the effective rigidity of such a plate, we can introduce a non-linear rigidity function $\tilde{D} = \tilde{D}(\phi)$ such as

$$\tilde{D}(\phi)\frac{\partial^2 w(x)}{\partial x^2} \approx -\tilde{D}(\phi) R_{xy}^{-1} = -\tilde{M}_x(\phi). \tag{A3}$$

Accordingly, we define the effective elastic thickness $\tilde{T}_e = \tilde{T}_e(\phi)$ as

$$\tilde{T}_e = \left[\frac{\tilde{D}(\phi)}{L}\right]^{1/3} = \left[-\frac{\tilde{M}_x(\phi) R_{xy}}{L}\right]^{1/3} \approx \left\{\frac{\tilde{M}_x(\phi)}{L}\left[\frac{\partial^2 w(x)}{\partial x^2}\right]^{-1}\right\}^{1/3}, \tag{A4}$$

where $L = E[12(1 - \nu^2)]^{-1}$ is defined for some reference values of E and ν (see above), and $R_{xy} \approx -(w'')^{-1}$ is the radius of plate curvature. The effective rigidity $\tilde{D}$ and effective elastic thickness $\tilde{T}_e$ can be obtained from the solution of the system (A1) and equilibrium equation (A2) with relations between stresses σ_{xx} and strains $\varepsilon_{xx} = \varepsilon_{xx}(\phi)$ in (A1) defined according to the constitutional laws (2.1–2.5).